

Oogenesis, spermatogenesis and spermiation structures in Lake Tanganyika Synodontis species (Mochokidae, Telostei: Siluriformes)

Authors: Dyková, Iva, Žák, Jakub, Blažek, Radim, Zimmermann, Holger, Polačik, Matej, et al.

Source: Journal of Vertebrate Biology, 73(24023)

Published By: Institute of Vertebrate Biology, Czech Academy of Sciences

URL: <https://doi.org/10.25225/jvb.24023>

BioOne Complete (complete.BioOne.org) is a full-text database of 200 subscribed and open-access titles in the biological, ecological, and environmental sciences published by nonprofit societies, associations, museums, institutions, and presses.

Your use of this PDF, the BioOne Complete website, and all posted and associated content indicates your acceptance of BioOne's Terms of Use, available at www.bioone.org/terms-of-use.

Usage of BioOne Complete content is strictly limited to personal, educational, and non - commercial use. Commercial inquiries or rights and permissions requests should be directed to the individual publisher as copyright holder.

BioOne sees sustainable scholarly publishing as an inherently collaborative enterprise connecting authors, nonprofit publishers, academic institutions, research libraries, and research funders in the common goal of maximizing access to critical research.

Oogenesis, spermatogenesis and spermiation structures in Lake Tanganyika *Synodontis* species (Mochokidae, Telostei: Siluriformes)

Iva DYKOVÁ^{1*} , Jakub ŽÁK^{1,2} , Radim BLAŽEK^{1,2} , Holger ZIMMERMANN^{2,3} ,
Matej POLAČIK² , Veronika BARTÁKOVÁ²  and Martin REICHARD^{1,2,4} 

¹ Department of Botany and Zoology, Faculty of Science, Masaryk University, Brno, Czech Republic; e-mail: dykova.iva@gmail.com, fish.jakub.zak@gmail.com, blazek@ivb.cz, reichard@ivb.cz

² Institute of Vertebrate Biology of the Czech Academy of Sciences, Brno, Czech Republic; e-mail: polacik@ivb.cz, bartakova.v@ivb.cz

³ University of Graz, Institute of Biology, Graz, Austria; e-mail: holger.zimmermann@uni-graz.at

⁴ University of Łódź, Department of Ecology and Vertebrate Zoology, Łódź, Poland

► Received 25 February 2024; Accepted 28 March 2024; Published online 25 April 2024

Abstract. *Synodontis* catfishes in Lake Tanganyika have undergone a modest radiation, with differences among species in reproductive strategies, including one species that has evolved to be an obligate brood parasite. Here, we provide insights into the reproductive traits and histology of male and female reproductive organs of five Lake Tanganyika *Synodontis* species (*S. irsacae*, *S. melanostictus*, *S. multipunctatus*, *S. petricola* and *S. polli*). We describe the structures employed in oogenesis, spermiogenesis and spermiation. We show that the shape and size of the urogenital papilla is a valuable trait for sex determination in all species except *S. polli*, where the imprecision reached > 20 %. From a histological perspective, the inter-specific structural differences associated with the type of reproductive strategy were not found in the ovaries. However, testicular histology indicated variations in spermiation structures among species, namely in *S. multipunctatus* and *S. irsacae*. The differences identified may be related to variation in reproductive strategies among species. In particular, weaker eosinophilia of testicular secretions was found in *S. multipunctatus* than in other species, suggesting the possibility of a different composition. Experimental manipulation of environmental and hormonal stimuli represents a promising direction for further research into the structural and functional diversity of male gonads in *Synodontis* species from Lake Tanganyika.

Key words: cuckoo catfish, gonad histology, ovaries, testes

Introduction

Evolutionary radiations arise when diversification and speciation are driven by expansion to new geographical areas or niche space (Rundell & Price 2009, Simões et al. 2016). Ancient lakes are typical island-type habitats where radiations can take place.

Lake Tanganyika in equatorial Africa harbours several smaller and larger evolutionary radiations (Salzburger et al. 2014), including a flock of several *Synodontis* catfish species (Day et al. 2009). The extent to which Lake Tanganyika *Synodontis* spp. differ from each other in ecological and life history traits is largely unknown, except that one species, *S. multipunctatus*,

* Corresponding Author



is an obligate brood parasite of mouthbrooding cichlids (Sato 1986), while the other species appear to scatter their eggs in and above rock crevices. Brood parasitism requires modifications in reproductive traits, from seasonal patterns of reproduction and frequency of egg laying to traits associated with reproductive behaviour (Spottiswoode et al. 2012). These adaptations may be reflected in the structure of gonads and their accessory glands.

The present study investigates the morphology of reproductive traits and structures, with emphasis on oogenesis, spermatogenesis and spermiation in five species of *Synodontis* from Lake Tanganyika collected in the field during two separate seasons. We compared our data with previous accounts on gonads of various teleost fishes, with a particular focus on closely related species. The general interpretation of the histological analysis of *Synodontis* gonads was assisted by comprehensive reviews of Chowdhury & Joy (2007), Schulz & Nóbrega (2011), Nishimura & Tanaka (2014), Uribe et al. (2014) and Pecio (2019). Important details were previously reported in studies on catfishes, especially on *Clarias* spp. (Siluriformes) were studied in relation to their reproductive strategies (e.g. Van den Hurk et al. 1987, Melo et al. 2011, Zakariah et al. 2016). For the gonadal structure of *Synodontis* spp., incomplete data are available for *S. eupterus* studied by Shinkafi & Daneji (2011). Other studies on particular *Synodontis* species focused mainly on the biological characteristics of their reproduction (Olatunde 1989, Laleye et al. 2006, Yongo & Wairimu 2018) rather than gonad structure. To the best of our knowledge, there are no previous studies of the gonadal structure of the *Synodontis* species included in the present study.

Material and Methods

Examined material

A total of 127 females and 114 males of wild *Synodontis* spp. (*S. irsacae*, *S. melanostictus*, *S. multipunctatus*, *S. petricola* and *S. polli*) were included in the present study for histological examination (Table 1). The original dataset included three *S. irsacae* males, one *S. melanostictus* female and one *S. multipunctatus* female, which were unavailable for histological examination due to technical issues, reducing the total sample of wild fish to 241. Wild fish were caught using a hand net during scuba diving or collected in minnow traps in the southern part of Lake Tanganyika, Zambia (9 km perimeter, 8°43'47.2" S 31°09'24.6" E; collection permit: K-4335/18 KA/K.48/18). The sampling was conducted in two different seasons: the dry season (October 2021) and the rainy season (March 2022), and the samples were distributed equally among both seasons. Fish examined in the present study were the subsample of the largest caught individuals of each sex-species-season combination from the total sample of wild-caught fish. Wild fish material was supplemented with three male *S. multipunctatus* (90-100 mm TL) maintained from hatching up to the age of four years in the breeding facility of the Institute of Vertebrate Biology, CAS Brno (accreditation 52699/2018-MZE-17214). The number of individuals examined per species and year of collection are summarized in Table 1.

The sex of each fish was first visually determined from the size and shape of the urogenital papilla (Cavaco et al. 1998; Fig. 1) upon collection by an expert (R. Blažek) and then confirmed by histological examination. The concordance between the visual

Table 1. Overview of the sample characteristics and sex determination precision of five *Synodontis* species (*S. irsacae*, *S. melanostictus*, *S. multipunctatus*, *S. petricola*, *S. polli*) from the Lake Tanganyika. Only individuals where it was possible to gather histological information are included. There were only three individuals of *S. melanostictus*, therefore only the sample characteristics are presented. Values in brackets are SE if not specified differently. Different superscript letters (^{a, b} when present) represent significant differences among species.

Species	Total individuals (2021, 2022)*	Body size (mean, min-max, mm)	Error in the sex determination by urogenital papilla (%)
<i>S. irsacae</i>	53 (25, 28)	98, 75-142	2.5 (1.7) ^b
<i>S. melanostictus</i>	3 (0, 3)	190, 173-208	NA
<i>S. multipunctatus</i>	59 (30, 29)	81, 67-100	1.5 (1.2) ^b
<i>S. petricola</i>	60 (29, 31)	93, 72-120	0.3 (0.3) ^b
<i>S. polli</i>	65 (34, 31)	124, 96-161	22.8 (11.8) ^a

* Sample size for wild-caught fish only (i.e. three *S. multipunctatus* from captivity are excluded).



Table 2. The results of a Generalized Linear Model with binomial error distribution for the precision of visual sex determination based on the shape of urogenital papillae. The visually determined sex was compared to gonad histology. *Synodontis polli* is set as a reference level to which other coefficients are compared. SE is the standard error of the mean. Values are on a logit scale.

Coefficients	Estimate	SE	z-value	P
Intercept	9.576	3.444	2.780	0.005
Sex	-2.200	0.778	-2.829	0.004
<i>S. irsacae</i>	-2.438	1.034	-2.357	0.018
<i>S. multipunctatus</i>	-2.994	1.206	-2.482	0.013
<i>S. petricola</i>	-4.742	1.438	-3.297	0.001
TL	-0.097	0.030	-3.213	0.001

inspection and histological assessment was tested by a generalised linear model (GLM) with binomial error distribution with a logit-link function. The agreement between visual inspection and histological assessment (1-concordance, 0-discordance) was fitted as the response variable and species (4-level factor), sex (male or female as determined by histology, 2-level factor) and body length (TL: from snout to the tip of the caudal fin, continuous) as predictors. Tukey *post-hoc* comparisons were performed with emmeans v 1.5.4 (Lenth 2021). The full model contained all possible pairwise interactions (sex:species; sex:TL; species:TL), but all were subsequently dropped as they were not significant ($P > 0.31$). The total sample size was 242 because all four *S. melanostictus* were excluded from this analysis due to the low sample size, and it was possible to determine sex (but no other histological information) from slides with technical issues.

Histology

All wild-caught fish were euthanised in clove oil and fixed in 10% neutral buffered formalin, with the belly opened ventrally to facilitate fixative penetration to internal organs. In the laboratory, fish were dissected, gonads of males and females were separated from other viscera and weighed to the nearest 0.01 g. The left and right ovaries were weighed separately to assess potential differences in mass. Their mass was compared by fitting a Linear Mixed Effect Model (LMME) from the lme4 package v 1.1.26 (Bates et al. 2015). Individual ovary mass was the response variable, and ovary side (left or right, factor) and its interaction with species (4-level factor) were included as predictors. Individual fish ID was included as a random factor to correct for the dependency of measurements within each individual. All statistical analyses were performed in the R environment v 4.2.2 (R Core Team 2022).

Whole testes and right ovary were then submerged into 70% ethanol and processed by the standard

paraffin technique using Histoplast (Sigma) as an embedding material. The standard fixative procedure for fresh organs removed from euthanized fish was applied to three fish from the breeding facility. Multiple (60-80) semi-serial sections were examined from each block. The oogenesis and spermiogenesis staging followed widely accepted criteria of Grier (1981) and Grier et al. (2009, 2018) related to the terminology of reproductive phases (as standardized by Brown-Peterson et al. 2011). Tissue samples of *Synodontis* gonads were subjected to a two-step examination, a non-targeted screening of the whole assemblage of *Synodontis* species aimed at identification of common and contrasting structural features and a second step focused on species-specific features.

Results and Discussion

Precision of the visual sex determination

The visual identification of sex by inspection of their urogenital papilla was less precise in females (GLM, back-transformed model estimated mean of error rate 6.5%, (SE = 2.6%), $z = 2.83$, $P = 0.004$, $n = 242$) than in males (0.8%, SE = 0.6%), and in smaller individuals (Table 2). The lower precision of sex determination in females may be ascribed to the shape similarity of papillae between subadults and females. At the species level, *S. polli* was the most difficult species for identification of its sex upon visual examination of the urogenital papilla (back-transformed model estimated mean of error rate: 22.8% (SE = 11.8%)) and tended to be significant from other species (Tukey *post hoc* pairwise comparisons from binomial GLM, all $z > 2.36$, $P = 0.005-0.08$). All other species (*S. irsacae*, *S. multipunctatus*, *S. petricola*) had an error rate < 2.5%, which did not differ significantly among each other (all $P = 0.207-0.882$, Table 1). The lower success of visual sex identification in *S. polli* comes from less developed inter-sexual differences in the shape of urogenital papillae in small adults of this species. The results are in accordance with our



personal experience, where sex determination from the shape of the urogenital papilla is relatively easy in *S. multipunctatus* and *S. petricola*. In contrast, in *S. irsacae*, it is difficult (but still feasible), and it appears not to be a useful character for sex determination in *S. polli*, except in large (> 150 mm) individuals.

Maturation and reproductive state

Of 241 histologically examined individuals, 199 contained mature gametes in their gonads. The other 38 were likely adults but outside their reproductive state, as their gonads contained multiple developmental stages of gametes, or they were also considerably (> 5 mm) larger than the smallest individuals with the presence of mature gametes in gonads. For example, there was one *S. polli* male with the exclusive presence of spermatogonia in the testes, but it was likely an adult outside the reproductive phase due to its relatively large size (TL = 115 mm). The remaining four individuals of *Synodontis* spp. were likely subadults; they were small (at the lower range of total size of examined fish) and had small gonads with exclusive presence of the earliest developmental stage of gametes (oogonia: 1 × *S. multipunctatus*, TL = 67 mm; 1 × *S. irsacae*, TL = 82 mm; spermatogonia: 1 × *S. irsacae*, TL = 78 mm; 1 × *S. polli*, TL = 98 mm).

Gross morphology of ovaries

Data on the shape, size, and colour of organs from dissected fresh material (commonly used for a simple gross evaluation of gonad developmental stages) were not available for an adequate number of individuals. Therefore, our description is based on detailed observations of organs preserved in formaldehyde solution.

The ovaries, which are not always of equal shape, are a ventrally positioned paired organ with a slightly compressed left side to fit within the body cavity with the gut (Fig. 2a, b). The difference between the left and right ovaries is only in their shapes since their mass did not differ (LME, $\chi^2_1 = 1.01$, $P = 0.316$) and was consistent among species; the interaction term between ovary side and species was not significant ($\chi^2_3 = 1.16$, $P = 0.763$). In all studied species, the ovaries were sacculiform, narrowed caudally and joined at their posterior end to form a single common oviduct terminating at the urogenital pore. Most ovaries included oocytes at variable maturity stages in a similar ratio, except *S. irsacae*, where late vitellogenic stages of oocytes (when present) were the dominant maturity stage. In such cases, middle oocyte maturity stages were in the minority, and oogonia and primary oocytes were primarily the

other oocyte stages present. The dominance of late vitellogenic stages in *S. irsacae* was recorded in the rainy season of 2022 (13/14) but not in the dry season of 2021 (0/13). This observation indicated that, in contrast to the other species examined, *S. irsacae* has seasonal reproduction.

Gross morphology of testes

The testes were observed as a flat, bilaterally symmetrical organ with uneven lateral outlines. Separated from surrounding connective tissue, the lobate shape of the testes was seen in a large flat anterior part (Fig. 2c, d), whereas a caudal part resembled catfish seminal vesicles documented macroscopically in catfishes from the family Clariidae (Van den Hurk et al. 1987) and Auchenipteridae (Meisner et al. 2000).

Light microscopy of ovaries

The ovaries of the study species shared features standard to the ovaries of most teleost fishes. They were covered with connective tissue, walls subdivided by ovigerous lamellae/folds, in which oogenesis started with the proliferation of oogonia/oogonia stem cells. Oogonia were round; their cytoplasm was pale, and a large diameter nucleus contained a prominent nucleolus (Fig. 3a, b). Formed by the mitotic division of much smaller germ cells (difficult to demonstrate in histological sections), oogonia were grouped in nests located under the wall of ovaries and in ovigerous lamellae protruding into deep layers of this organ. Oogonia differed substantially from the next stage of oogenesis, i.e. from primary oocytes with strongly basophilic cytoplasm (Fig. 3b-e). This stage transformed into early oocytes characterized by an increased volume of cytoplasm with Balbiani bodies (e.g. Schisa 2012) and round nuclei that contained nucleoli on their periphery (Fig. 3c, d). Early oocytes were covered by a delicate structure comprising a simple layer of squamous follicle cells. Oogonia and primary oocytes belonging to the previtellogenic stages of ovarian development were usually found together with advanced, i.e. vitellogenic, stages. Unlike in previtellogenic stages, the cytoplasm of early vitellogenic oocytes was pale and contained numerous tiny yolk droplets densely accumulated around the nucleus, whereas the peripheral part of the cytoplasm contained numerous vacuoles, also called vesicles or cortical alveoli (Fig. 4a-d). In advanced vitellogenesis, the oocytes are enlarged due to the progressive accumulation of yolk substances and the growth of yolk droplets/globules. The oocyte membrane differentiated to form a well-visible layer called zona radiata (a term used in original papers



and fish histology textbooks due to its radial striations described at the subcellular level: Chaudhry 1956, Anderson 1967, Flügel 1967, Matsuyama et al. 1991). Note that zona radiata is termed zona pellucida in mammalian histology textbooks. The follicle cells surrounding the zona radiata, which were initially flat/squamous, became cuboid, contained prominent nuclei and formed continuous oocyte envelope (Fig. 4d, e). In the course of oocyte late vitellogenesis, follicle cells increased in size, became cylindrical and underwent conspicuous changes manifested by the presence of multiple vacuoles in their cytoplasm and the loss of staining properties (Fig. 5). The comparison of *Synodontis* vitellogenic oocytes revealed a direct correlation between the stage of vitellogenesis as manifested by the size of yolk globules and the morphology of follicular layer. In oocytes with the largest yolk globules, the most advanced changes in the follicular layer were seen in terms of increasing cell height, increased vacuolization of cell cytoplasm, and loss of cell stainability (Fig. 5). Similar changes of follicular layer were documented in Neotropical catfishes (Melo et al. 2011) which linked follicle cell characteristics to their reproductive strategies (pelagic spawners, demersal spawners, and internally fertilizing species). Unfortunately, no data were available about the exact synchronisation of the vitellogenic stages used for comparison with histometric data collected on follicular cells.

The post-ovulatory fate of follicular cells has rarely been addressed. Shelton (1978) summarized varieties of development and transformation of follicular cells in fishes and described in detail the contribution of follicular cells persisting after ovulation to egg adhesiveness in the clupeid fish *Dorosoma petenense*. A comparison of the most developed ovarian oocytes of *S. multipunctatus* collected in the wild with eggs of the same species produced in the laboratory during artificial reproduction by applying gentle pressure on the abdominal cavity (Blažek et al. 2018) revealed the absence of cellular follicular envelope in artificially spawned eggs. Under the light microscope, the zona radiata of artificially spawned eggs was covered with a layer of homogeneous acellular material (Fig. 6c, d) considered to be a product of follicular cells in most bony fishes (Shelton 1978). Similar advanced transformation of the cellular follicular envelope into a homogeneous acellular layer was observed in intraovarian oocytes of two *S. polli* individuals of this study (Fig. 6a, b).

Histological evaluation of the female reproductive development in *Synodontis* spp. identified

previtellogenic stages of oogenesis in 14 out of 66 females collected in October 2021. This means that 21% of females were not in a reproductive phase (2/14 *S. polli*, 9/14 *S. irsacae*, 3/14 *S. multipunctatus*). The examination of females collected in March 2022 revealed exclusively the co-occurrence of early and late vitellogenic oocyte stages; hence, all those females were developmentally mature and soon prepared to spawn.

The oocyte dysmorphism (Fig. 7) was found in all four *Synodontis* species (technical issues prevented examination of a single *S. melanostictus*) – in one female (*S. polli*) in 2021 (out of 66 examined females of all *Synodontis* spp.) and 13 (out of 59) females in the 2022 dataset. Overall, oocyte dysmorphism was identified in 4/27 *S. irsacae*, 2/34 *S. multipunctatus*, 3/30 *S. petricola* and 4/34 *S. polli*. This aberrant oocyte morphology linked to an atypical course of meiosis was classified as irreparable, i.e. meiotic resumption was not expected.

Ovarian regressive changes such as those affecting oviducts, the presence of so-called postovulatory follicles (reported, e.g. in siluriform fish by Sales et al. 2016) and atretic oocytes, were difficult to estimate accurately in *Synodontis* spp., due to low general cohesion of ovarian tissues and multiple artefacts arising from sectioning mature oocytes containing large yolk globules (Fig. 6e and Fig. 8).

Unusual ovarian cellularity, presumably representing an inflammatory response, was found in three individuals (*S. polli*, *S. irsacae* and *S. multipunctatus*) in association with cross-sections of unidentifiable nematodes localized in the abdominal cavity (Fig. 9).

In summary, the comparison of oogenesis structures revealed no significant differences among the study species. Based on the material examined, a single finding of an advanced degree of intraovarian follicular layer transformation cannot be considered species-specific.

Light microscopy of testes

The histology of male gonads was more difficult to investigate than that of females. Well-visible lobes of the anterior spermatogenic part of testes represented incompletely divided segments of left and right parts fused near the system of efferent ducts (Fig. 10). In all study species, testes structure corresponded to the unrestricted type *sensu* Grier (1981) and Uribe et al. (2014). Consequently, spermatogonia developed along the entire length of seminiferous tubules.



The earliest stage of spermiogenesis, i.e. exclusive occurrence of germinal primordia with proliferating spermatogonia, was detected in only two individuals (one *S. polli* and one *S. irsacae*) (Fig. 11). In all other individuals, more advanced stages of the gonadal development with spermatogonia, spermatocytes, spermatids and spermatozoa in seminiferous tubules were found so that these fish could be considered maturing or mature (Figs. 12-14). A pronounced dominance of either early or advanced spermatogenic stages was observed in 45 of 114 examined males. Among those, spermatogonia, spermatocytes and spermatids dominated in five of 45 males, while spermatozoa dominated in 40 of 45 males. Testes of the 69 remaining individuals contained all developmental stages without an apparent dominance.

Pronounced differences were observed among particular lobes of testes (Fig. 15). In tubules of some lobes, spermatogonia plus spermatocytes and spermatids prevailed; other lobes had tubules filled with spermatozoa and rarely earlier spermatogenic stages or with eosinophilic material considered testicular plasma *sensu* Mansour et al. (2004). Three individuals of *S. multipunctatus* reared under laboratory conditions for four years were additionally examined, and all showed signs of advanced stage of maturity. Like individuals from the wild, laboratory-reared individuals had asynchronous development of testicular lobes.

The anterior part of the efferent system of male gonads with efferent ductules of individual lobes collecting and emptying spermatozoa to bilateral main testicular/efferent ducts (Fig. 16) was relatively easy to follow. The posterior part of the efferent system with sperm duct was observed in a preserved condition only exceptionally (Fig. 10). The site of the testicular duct connection is missing in the documentation due to the intricate architecture of the posterior part of the testes. The structure of efferent ductules and duct walls is presented in Fig. 16.

Interpretation of the structure in the posterior part of the testes, referred to as seminal vesicles, accessory glandular organ or sperm duct glands in Siluriformes and many other teleosts (Miller 1992, Chowdhury & Joy 2007), was even more difficult than that of the anterior spermiogenic part. Adequate histological description was possible only for some of the diverse functions attributed to the fish seminal vesicles (Chowdhury & Joy 2007, Schulz & Nóbrega 2011, Uribe et al. 2014). In our *Synodontis* dataset, seminal vesicles principally served to store accumulated

spermatozoa prior to their release for fertilization. Histological observation of the secretory activity of epithelial cells that participate in seminal vesicle fluid production was feasible but challenging due to the topography of this part of testes, spatial arrangement of vesicles (well seen in gross morphology of large individuals), and challenging removal of this fragile organ for a detailed study.

In most *Synodontis* males, multi-chambered vesicles with spermatogenic stages in various densities predominated in the posterior part of the testes (Figs. 17-22). Although frequently observed in fragments, they evidently functioned as seminal vesicles, i.e. repositories/storage places of most advanced spermatogenic stages. In our histological sections, whether these vesicles contained exclusively mature spermatozoa or also advanced spermatids could not be identified with certainty. In some vesicles, spermatozoa were mixed with material of pronounced eosinophilia, also reported as seminal vesicle plasma, a supposed component of seminal vesicle fluid. Co-occurrence of vesicles containing spermatozoa and those also containing eosinophilic material was registered in the caudal part of the testes in 31 of 114 *Synodontis* spp. males under study (5/26 *S. irsacae*, 2/3 *S. melanostictus*, 4/25 *S. multipunctatus*, 11/30 *S. petricola*, 9/30 *S. polli*).

Posterior vesicles with the structural characteristics of an active secretory gland, similar to those reported in the comprehensive review by Chowdhury & Joy (2007) across ten teleost families, were found only in two individuals (*S. irsacae* and *S. melanostictus*). We, therefore, cannot confirm whether this is a typical structure in the examined species. Interconnected chambers of these vesicles were lined by simple cuboidal epithelium and contained acellular homogeneous acidophilic/eosinophilic material. A special situation – all vesicles of the posterior part of the testes being filled with seminal vesicle secretion/plasma – was found in one fish, *S. melanostictus* (Fig. 20).

In other instances, vesicles containing eosinophilic material (5/26 in *S. irsacae*, 1/3 in *S. melanostictus*, 15/30 in *S. polli*) differed in having small to large clusters of spermatozoa (Fig. 18a, b) within a predominating eosinophilic content. Flocculated or dense eosinophilic content was found only in several cases (Fig. 18c). Atrophy of epithelial lining responsible for seminal vesicle secretion was found in *S. polli* (Fig. 18d). Histological study can hardly determine composition of eosinophilic materials and



relate their appearance in sections with results of detailed mucopolysaccharide-protein-lipid analyses reported in other fish species (Chowdhury & Joy 2007). Nevertheless, the density of seminal vesicle contents could be inferred from sections stained with Hematoxylin and Eosin (H & E). The liquid content of vesicles was washed out during the processing of tissue samples, leaving them empty (Fig. 22c), whereas dense and strongly eosinophilic material remained embedded in vesicles (Figs. 17, 18).

Solitary ducts filled with dense eosinophilic material were interposed between posterior seminal vesicles near the long axis of the testes and suggested to be part of the sperm duct gland. However, the site of connection with the sperm duct was not found.

In teleost fish, seminal vesicle variability and temporal changes in their morphology were always related to cycling changes (Chowdhury & Joy 2007). However, studies focused on experimentally induced changes are rare.

Comments on male gonads of individual *Synodontis* species

Synodontis irsacae

The set, initially comprising 29 individuals, was reduced to 26 due to technical issues. Five individuals were outside their spawning season and/or immature, with very small spermiogenic lobes. Nineteen individuals were available for histological assessment of most parts of the testes. Contrary to males of the other examined species, *S. irsacae* males possessed, in addition to spermiogenic lobes, lobes containing slightly eosinophilic secretion (testicular fluid/testicular plasma) in the anterior and middle parts of testes. The revision of epithelial linings ruled out the possibility that these tubules were mistaken for 'spent' spermiogenic lobes. High magnification of selected transverse sections links this finding of secretory tubules to those observed in *S. melanostictus*. Multichambered storage vesicles containing spermatozoa mixed with strongly eosinophilic material were found in the posterior part of the testes in seven individuals. Selected details are presented in Fig. 19.

Synodontis melanostictus

This species was represented by only three individuals but considerably contributed to the knowledge of male gonad accessory structures. One individual was not in a reproductive phase and had only small spermiogenic lobes in their initial stage of development. Spermiogenic lobes of the other two males resembled the regenerated phase with some

developmental stages in the tubular epithelium and a minimum number of luminal spermatozoa. The posterior testicular part of these individuals was furnished with secretory vesicles of uniform shape and well-preserved structure. The contents of vesicles were strongly eosinophilic, mostly homogeneous, and only rarely of clot consistency. Selected details are seen in Fig. 20.

Synodontis multipunctatus

Male gonads of 25 individuals collected in the wild and three from laboratory breeding were examined in numerous semi-serial sections to compare their structure with other *Synodontis* species included in the study. This species is an obligate brood parasite, and we predicted structural differences from other species due to its unique reproductive strategy (assuming permanent readiness to spawn and more frequent spawning bouts). Both wild and laboratory-bred individuals were characterized by advanced stages of spermiogenesis, the same type of multichambered seminal vesicles, and individual secretory tubules associated with seminal vesicles. Despite identical histological techniques applied, testicular secretions (testicular plasma and seminal vesicle plasma) of *S. multipunctatus* were characterized by the weaker eosinophilia than in other species, suggesting a different composition of testicular secretions. These findings appear relevant to the role of secretion in spermiation in terms of both development and sperm release in *S. multipunctatus*. No sperm duct gland was found in any *S. multipunctatus* despite a large number of thin semiserial sections examined. Some details are presented in Figs. 17-21 for interspecific comparison.

Synodontis petricola

A total of 30 individuals of the species were included in the study. The posterior part of the gonads was available for examination in 26 males. Seminal vesicles of 15 individuals were found almost 'empty' or with a minimum number of spermatozoa. The vesicles of two fish contained a medium-density mass of spermatozoites. Seminal vesicles of the remaining nine fish contained an eosinophilic precipitate with low numbers of admixed spermatozoites in chambers of seminal vesicles. Based on observations in other *Synodontis* species, it can be assumed that the original contents of seminal vesicles were more liquid than cellular and, thus, were easier to wash out in the course of processing for histology. The small volume and faint eosinophilia of secreted material support the prevailing idea of a storage function of the seminal vesicles in *S. petricola*. Details are included in Fig. 22.



Synodontis polli

Of the 30 individuals of this species identified for comparison of male gonad histology, two had only spermatogonial developmental stages in clumps and small spermatogenic lobes lacking lumina in seminiferous tubules, respectively. An asynchronous development of spermiogenic lobes characterized mature individuals in the spawning phase and showed a wide range of varieties in the posterior segment of testes. Seminal vesicles took the form of multi-chambered storage structures, with partitions between chambers covered with flat epithelium. The chamber contents varied in proportions of stored spermatozoa and eosinophilic secretion. The latter differed in its density, intensity of eosinophilia and structure (either homogeneous or coagulated/precipitated). Secretion significantly dominated the seminal vesicles of the majority of *S. polli* examined. A rare finding of a regressively altered vesicle was also recorded. Selected details are documented in Figs. 17 and 18.

General Discussion

We present a detailed histological investigation of female and male gonads to inform further investigations into the ecology and evolution of a modest lacustrine radiation of *Synodontis* spp., which includes an obligate brood parasitic species. *Synodontis irsacae* had features suggesting seasonal reproduction since its ovaries contained a late vitellogenetic stage; it was almost exclusively the dominant oocyte stage present in the ovary. Histology of reproductive organs of three other species appeared to produce mature gametes continuously (no pronounced seasonal pattern of reproduction). Overall, the assessment of oogenesis and spermiogenesis structures in a set of five *Synodontis* species 1) revealed a set of features shared across species and 2) identified the posterior part of testes as a source of interspecies variability. However, for species-specific structures, the results are less conclusive than predicted.

Testes, especially their posterior part, were more difficult for structural interpretation than ovaries. Histological sections of the integral undamaged posterior part of the testes were not available in a sufficient number of individuals. Obtaining the undamaged posterior part of the testes fixed either *in situ* (in the field) or during the dissection of fresh material (in the laboratory) was complicated due to the intricate topography of this part of the gonads, which can be easily damaged. When fixed *in situ*, it became tightly connected to the other organs. When it was

separated during the dissection of fresh material, it was even more vulnerable to structural damage. Due to these adverse technical circumstances, a series of issues important for quantifying potential variability in the posterior part of testes could not be obtained from histological examination of the material studied. They include 1) the presence (or absence) of a separate sperm duct gland, 2) the number of lobes with the supposed function of seminal vesicles, 3) whether the structure of individual lobes is permanent (or dynamic over days/weeks), 4) whether the number of seminal vesicles is stable after reaching maturity, and 5) whether and how seminal vesicles regenerate. Seminal vesicles were attributed to a variety of functions in most comprehensive reviews on teleost fish (Chowdhury & Joy 2007, Schulz & Nóbrega 2011, Uribe et al. 2014). We acknowledge that the evaluation of interspecific structural differences considered in our study is masked due to the very rapid dynamic of morphological changes, particularly those based on the activation of secretory cells via hormonal impulses. Artificial reproduction of Lake Tanganyika *Synodontis* catfishes is now successful (e.g. Kaiser & Rouhani 1999, Blažek et al. 2018). In the future, artificial reproduction could be employed for experimental work with fish in spawning condition. This approach would facilitate the experimental manipulation of environmental and hormonal stimuli, offering an opportunity to disentangle the issues above. This, in turn, could provide a more detailed understanding of the species-specific structural differences in the gonads of *Synodontis* spp.

Acknowledgements

Funding for this study came from the Czech Science Foundation (21-00788X). Holger Zimmermann was funded by the Austrian Science Fund (FWF, project nr. J 4584).

Author Contributions

Conceptualization: I. Dyková, M. Reichard, J. Žák; Methodology: I. Dyková, J. Žák; Validation: I. Dyková, J. Žák; Formal analysis: I. Dyková, J. Žák; Investigation: I. Dyková, J. Žák, R. Blažek; Resources: I. Dyková, R. Blažek, H. Zimmerman, M. Polačik, V. Bartáková, M. Reichard; Data curation: I. Dyková, J. Žák; Writing – Original Draft: I. Dyková, J. Žák, M. Reichard; Writing – Review and Editing: I. Dyková, J. Žák, R. Blažek, H. Zimmerman, M. Polačik, V. Bartáková, M. Reichard; Visualization: I. Dyková, H. Zimmerman, J. Žák, R. Blažek; Supervision: I. Dyková, M. Reichard; Funding acquisition: M. Reichard.



Literature

- Anderson E. 1967: The formation of the primary envelope during oocyte differentiation in teleosts. *J. Cell Biol.* 35: 193–212.
- Bates D., Maechler M., Bolker B. & Walker S. 2015: Fitting linear mixed-effects models using lme4. *J. Stat. Softw.* 67: 1–48.
- Blažek R., Polačik M., Smith C. et al. 2018: Success of cuckoo catfish brood parasitism reflects coevolutionary history and individual experience of their cichlid hosts. *Sci. Adv.* 4: eaar4380.
- Brown-Peterson N.J., Wyanski D.M., Saborido-Rey F. et al. 2011: A standardized terminology for describing reproductive development in fishes. *Mar. Coast. Fish.* 3: 52–70.
- Cavaco J., Eduardo B., Vilrocx C. et al. 1998: Sex steroids and the initiation of puberty in male African catfish (*Clarias gariepinus*). *Am. J. Physiol.* 275: R1793–R1802.
- Chaudhry H.S. 1956: The origin and structure of the zona pellucida in the ovarian eggs of teleosts. *Z. Zellforsch. Microsk. Anat.* 43: 478–485.
- Chowdhury I. & Joy K.P. 2007: Seminal vesicle and its role in the reproduction of teleosts. *Fish Physiol. Biochem.* 33: 383–398.
- Day J.J., Bills R. & Friel J.P. 2009: Lacustrine radiations in African *Synodontis* catfish. *J. Evol. Biol.* 22: 805–817.
- Flügel H. 1967: Licht-und elektronenmikroskopische Untersuchungen an Oozyten und Eiern einiger Knochenfische. *Z. Zellforsch. Microsk. Anat.* 83: 82–116.
- Grier H.J. 1981: Cellular organisation of the testis and spermatogenesis in fishes. *Am. Zool.* 21: 345–357.
- Grier H.J., Porak W.F., Carroll J. & Parenti L.R. 2018: Oocyte development and staging in the Florida bass, *Micropterus floridanus* (LeSuer, 1822), with comments on evolution of pelagic and demersal eggs in bony fishes. *Copeia* 106: 329–345.
- Grier H.J., Uribe M.C. & Patiño R. 2009: The ovary folliculogenesis, and oogenesis in teleosts. In: Jamieson B.G.M. (ed.), *Reproductive biology and phylogeny of fishes (Agnathans and Bony fishes)*, vol. 8A. *Science Publishers, Enfield, USA*: 25–84.
- Kaiser H. & Rouhani Q. 1999: Growth of juvenile *Synodontis petricola* (family: Mochokidae) fed on a formulated diet, *Artemia* or *Spirulina* and combinations thereof. *Aquar. Sci. Conserv.* 2: 117–123.
- Laleye P., Chikou A., Gnohossou P. et al. 2006: Studies on the biology of two species of catfish *Synodontis schall* and *Synodontis nigrita* (Ostariophysi: Mochokidae) from the Oueme River, Benin. *Belg. J. Zool.* 136: 193–201.
- Lenth R.V. 2021: emmeans: estimated marginal means, aka least-squares means. *R package version 1.5.4*. <https://github.com/rolenth/emmeans>
- Mansour N., Lahnsteiner F. & Patzner R.A. 2004: Seminal vesicle secretion of African catfish, its composition, its behaviour in water and saline solutions and its influence on gamete fertilizability. *J. Exp. Zool.* 301A: 745–755.
- Matsuyama M., Nagahama Y. & Matsuura S. 1991: Observations on ovarian follicle ultrastructure in the marine teleost, *Pagrus major*, during vitellogenesis and oocyte maturation. *Aquaculture* 92: 67–82.
- Meisner A.D., Burns J.R., Weitzman S.H. & Malabarba L.R. 2000: Morphology and histology of the male reproductive system in two species of internally inseminating South American catfishes, *Trachelyopterus luceani* and *T. galeatus* (Teleostei: Auchenipteridae). *J. Morphol.* 246: 131–141.
- Melo R.M.C., Arantes F.P., Sato Y. et al. 2011: Comparative morphology of the gonadal structure related to reproductive strategies in six species of neotropical catfishes (Teleostei: Siluriformes). *J. Morphol.* 272: 525–535.
- Miller P.J. 1992: The sperm duct gland: a visceral synapomorphy for gobioid fishes. *Copeia* 253–256.
- Nishimura T.G. & Tanaka M. 2014: Gonadal development in Fish. *Sex. Dev.* 8: 252–261.
- Olatunde A.A. 1989: Some aspects of the biology of *Synodontis shall* (Bloch-Schneider) in Zaria, Nigeria. *J. Aquat. Sci.* 4: 49–54.
- Pecio A. 2019: Testis structure, spermatogenesis, and spermatozoa in teleost fishes. In: Formicki K. & Kirschbaum F. (eds.), *The histology of fishes*, 1st ed. *CRC Press, Boca Raton, USA*: 177–206.
- R Core Team 2022: R: a language and environment for statistical computing. *R Foundation for Statistical Computing, Vienna, Austria*. <https://www.r-project.org/>
- Rundell R.J. & Price T.D. 2009: Adaptive radiation, nonadaptive radiation, ecological speciation and non ecological speciation. *Trends Ecol. Evol.* 24: 394–399.
- Sales C.F., Domingos F.F., Brighnetti L.S. et al. 2016: Biological variables of *Hypostomus francisci* (Siluriformes: Loricaridae) from Itapecerica River, Minas Gerais State, Brazil. *An. Acad. Bras. Cienc.* 88 (Suppl): 1603–1614.
- Salzburger W., Van Bocxlaer B. & Cohen A.S. 2014: Ecology and evolution of the African Great Lakes and their faunas. *Annu. Rev. Ecol. Evol. Syst.* 45: 519–545.



- Sato T. 1986: A brood parasitic catfish of mouthbrooding cichlid fishes in Lake Tanganyika. *Nature* 323: 58–59.
- Schisa J.A. 2012: New insights into the regulation of RNP granule assembly in oocytes. *Int. Rev. Cell Mol. Biol.* 295: 233–289.
- Schulz R.W. & Nóbrega R.H. 2011: Anatomy and histology of fish testis. In: Farrell A.P. (ed.), *Encyclopedia of fish physiology: from genome to environment*, vol. 1. Academic Press, San Diego, USA: 616–626.
- Shelton W.L. 1978: Fate of the follicular epithelium in *Dorosoma petenense* (Pisces: Clupeidae). *Copeia* 1978: 237–244.
- Shinkafi B.A. & Daneji A.I. 2011: Morphology of the gonads of *Synodontis eupterus* (Boulenger) from river Rima, North-western Nigeria. *Int. J. Zool. Res.* 7: 382–392.
- Simões M., Breitreuz L., Alvarado M. et al. 2016: The evolving theory of evolutionary radiations. *Trends Ecol. Evol.* 31: 27–34.
- Spottiswoode C.N., Kilner R.M. & Davies N.B. 2012: Brood parasitism. In: Royle N.J., Smiseth P.T. & Kolliker M. (eds.), *The evolution of parental care*. Oxford University Press, Oxford, UK: 226–356.
- Uribe M.C., Grier H.J. & Mejía-Roa V. 2014: Comparative testicular structure and spermatogenesis in bony fishes. *Spermatogenesis* 4: e983400.
- Van den Hurk R., Resink J.W. & Peute J. 1987: The seminal vesicle of the African catfish, *Clarias gariepinus*. *Cell Tissue Res.* 247: 573–582.
- Yongo E. & Wairimu A. 2018: Studies on the biology of *Synodontis victoriae* in the Nyanza Gulf of Lake Victoria, Kenya. *Fish. Aquac. J.* 9: 2.
- Zakariah M., Gambo B.G., Peter I.D. et al. 2016: Anatomical studies of the testes of wild African catfish (*Clarias gariepinus*) in spawning and non-spawning seasons in Maiduguri, Nigeria. *Int. J. Fish. Aquat. Stud.* 4: 272–277.

List of abbreviations

- DE – ductus efferent
 FL – follicular layer
 LC – Leydig cells
 OV – oviduct
 OW – ovary wall
 SD – sperm duct
 SIR – *Synodontis irsacae*
 SMP – *Synodontis multipunctatus*
 SMS – *Synodontis melanostictus*
 SPC – spermatocytes
 SPD – spermatids
 SPG – spermatogonia
 SPO – *Synodontis polli*
 SPT – *Synodontis petricola*
 SPZ – spermatozoa
 SV – seminal vesicle
 SVF – seminal vesicle fluid
 SVP – seminal vesicle plasma
 TP – testicular plasma

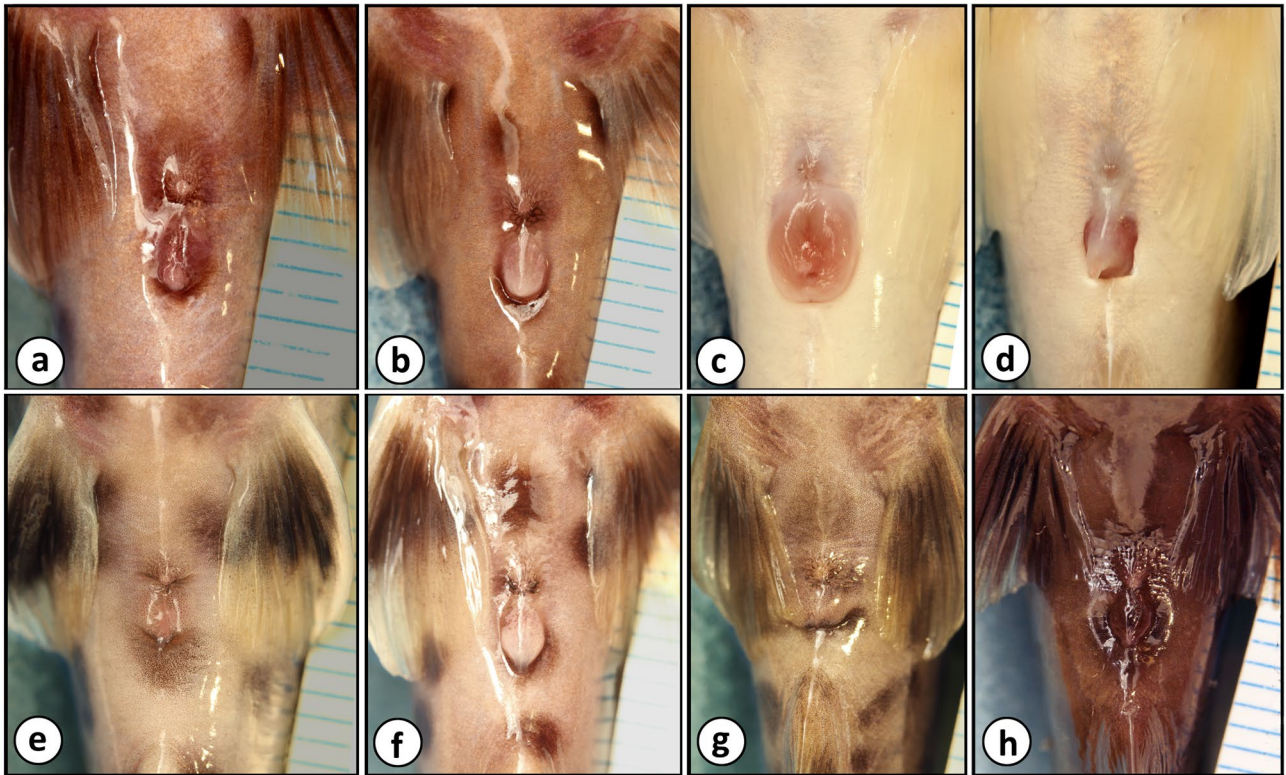


Fig. 1. Sex and species-specific shape of the urogenital papilla in four species of *Synodontis* spp. from Lake Tanganyika. a) *S. irsace* female. b) *S. irsace* male. c) *S. multipunctatus* female. d) *S. multipunctatus* male. e) *S. petricola* female. f) *S. petricola* male. g) *S. polli* female. h) *S. polli* male. Similarly sized individuals of each sex were photographed. Captive-bred individuals with well-developed sexual characters and known sex were photographed (photo Radim Blažek).

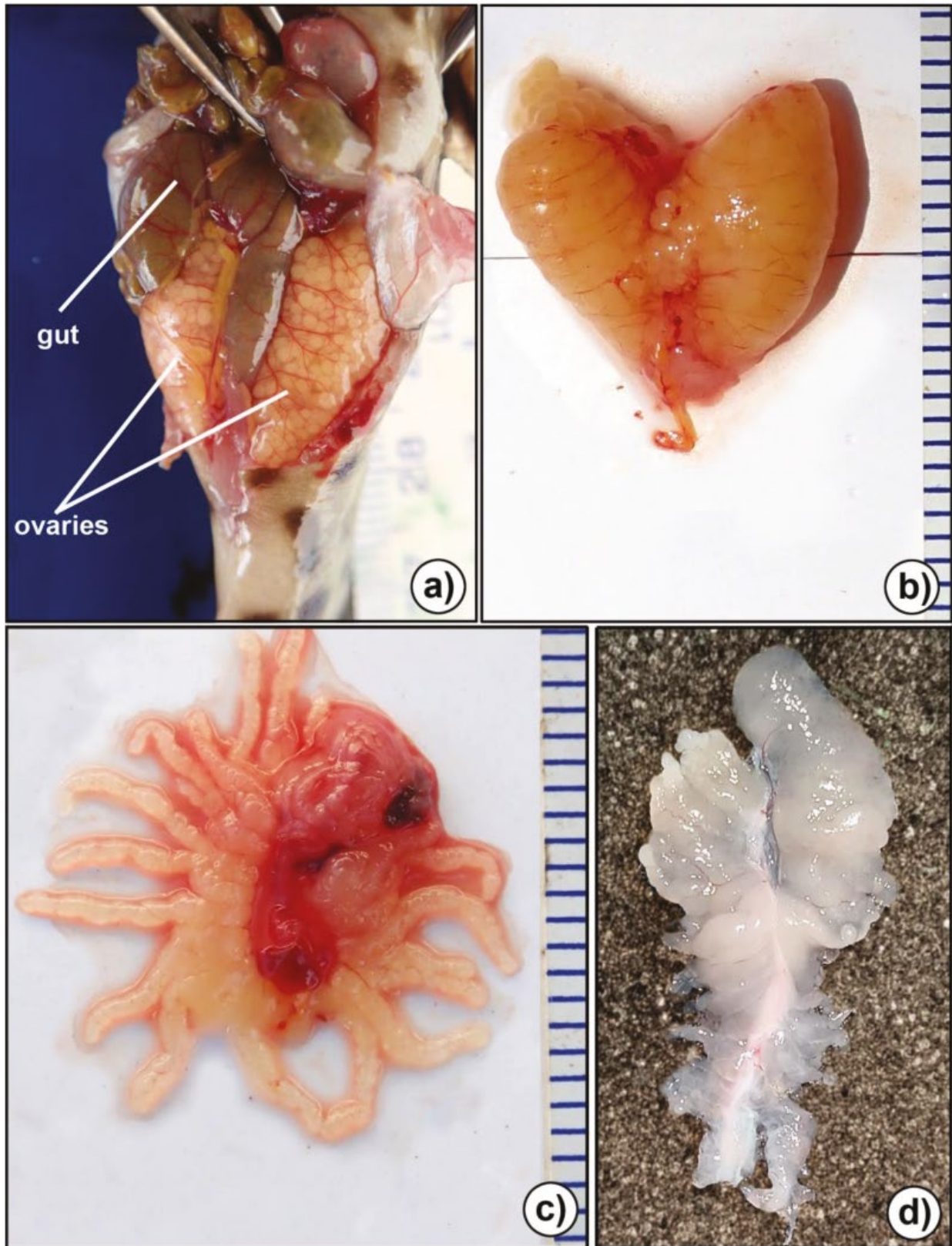


Fig. 2. Gonads of *Synodontis* sp. a) Position of ovaries in body cavity in relation to gut, wild *S. multipunctatus*, but the position of ovaries and their shape is identical to all five *Synodontis* spp. examined. Ovaries are asymmetrical in shape, but they have similar mass. b) Extracted ovaries from the body cavity of wild *S. multipunctatus*. c) Extracted testes from the body cavity of an individual from the wild. The finger-like projections in the caudal part of the testes are nicely apparent and are a feature of all testes within the five *Synodontis* spp. examined. The cranial part of the testes is slightly folded on the image due to technical difficulties and can be seen as red tissue (which comes with remnants of the kidney and gut). d) Extracted testes from 14 cm large captive-bred *S. multipunctatus*. All testes parts are apparent, but unfortunately, the lobate structure in the caudal part is less apparent due to technical difficulties. Images c) and d) provide a combined overview of the appearance of the testes. All figures are situated in cranial (top)-caudal (bottom) direction. Images are taken from wild-caught individuals. Individual side scale parts correspond to 1 mm.

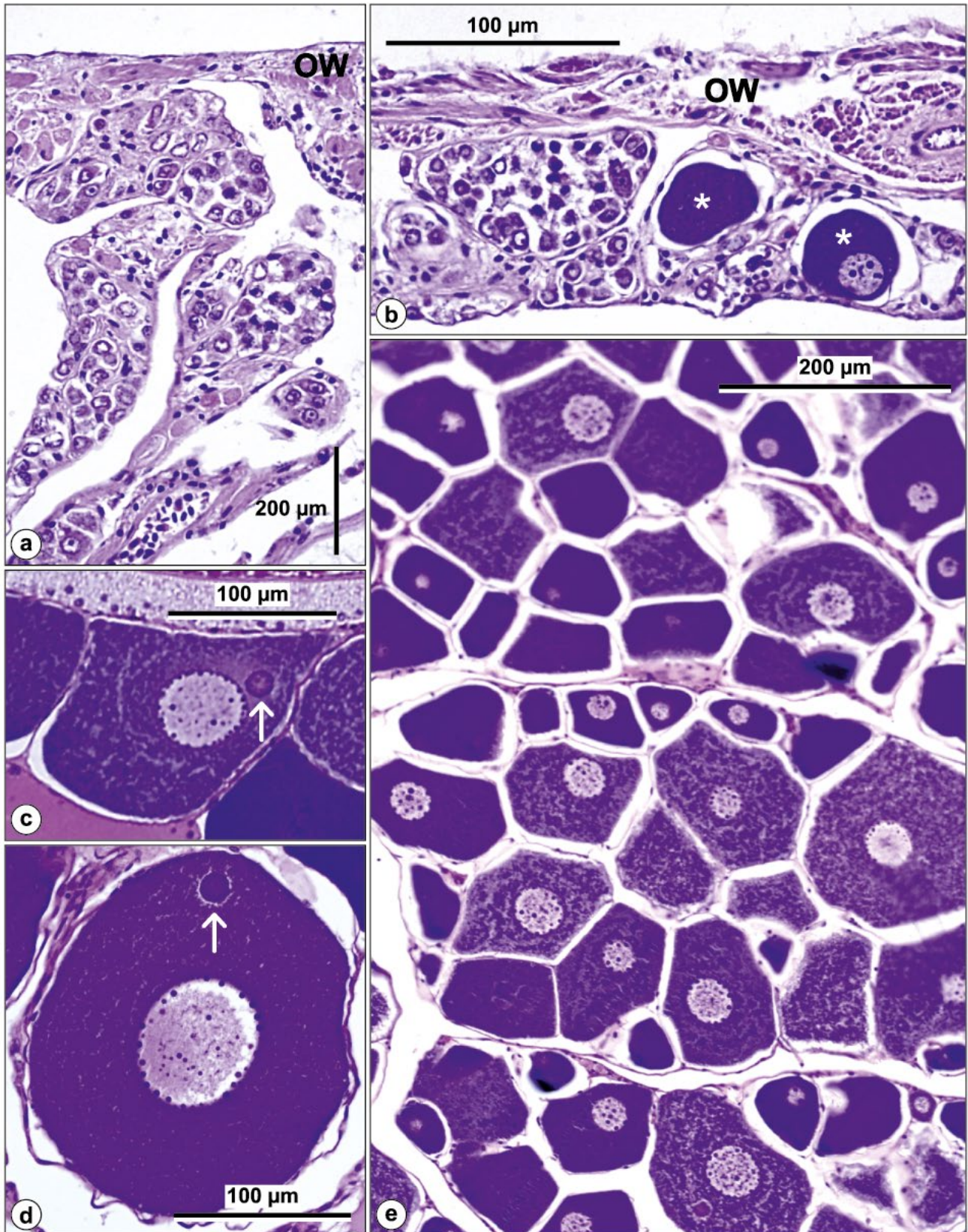


Fig. 3. Previtellogenic stages in the oogenesis of *Synodontis* spp. a), b) Oogonia proliferating in ovigerous lamellae interconnected with the ovary wall (OW) and primary oocytes (*) in b). (c-e) Primary oocytes with a delicate envelope of follicular cells differing in the size of profiles are shown in one plane of section, structure, and basophilia of the cytoplasm. Arrows mark Balbiani bodies in the cytoplasm of primary oocytes c), d). SPO a), b); SIR c), e); SMP d). H & E.

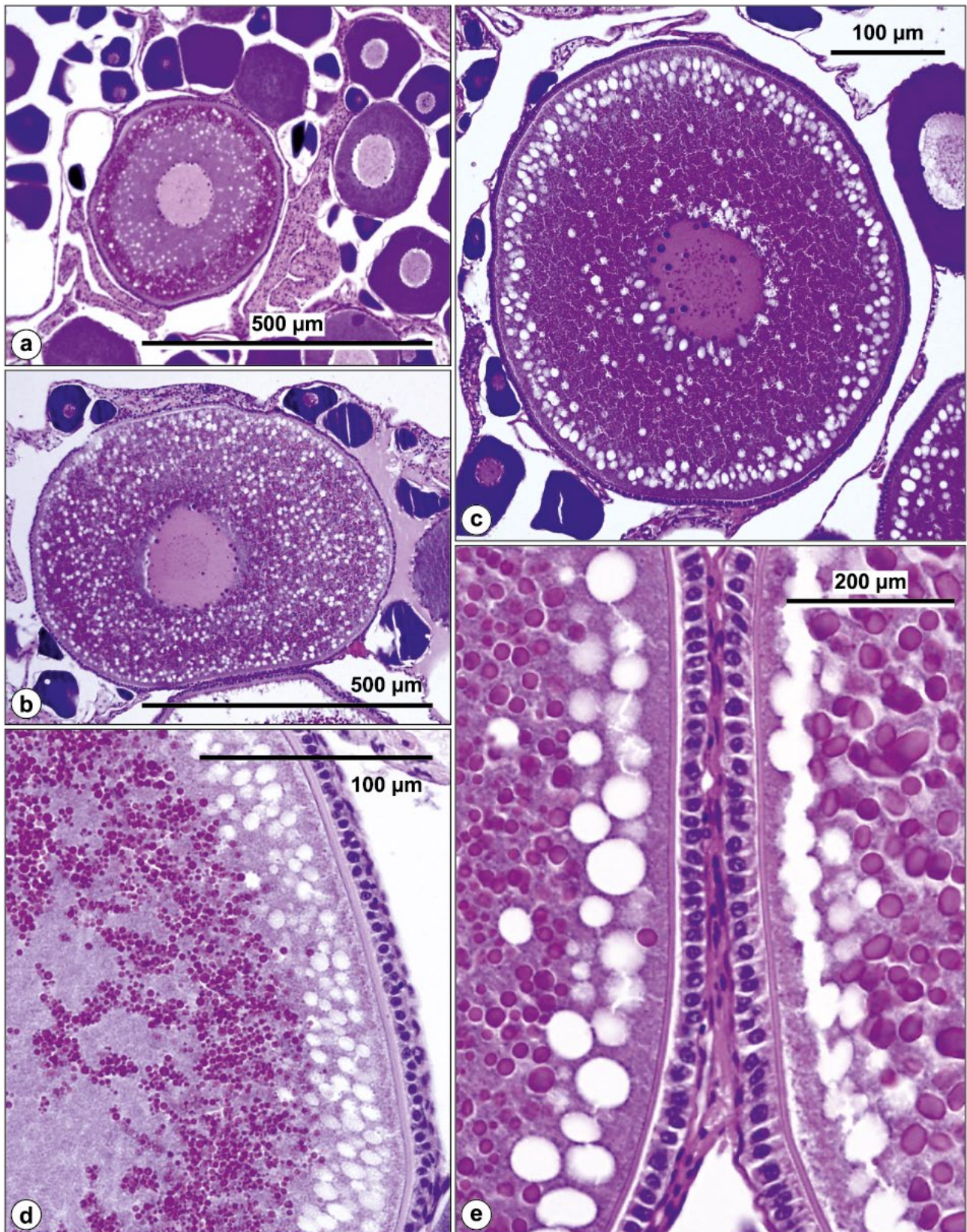


Fig. 4. Vitellogenic stages in *Synodontis* spp. oogenesis. (a-c) Early vitellogenic oocytes have small yolk droplets in the cytoplasm, and vacuoles are distributed evenly a), b) or accumulated on the periphery as 'cortical alveoli' c). d), e) Slightly advanced vitellogenic stages show the periphery of one d) and two neighbouring and apposed oocytes e) with a clearly distinguished layer of cubic follicular cells. SPT a); SMP b), d); SIR c); SPO e). H & E.

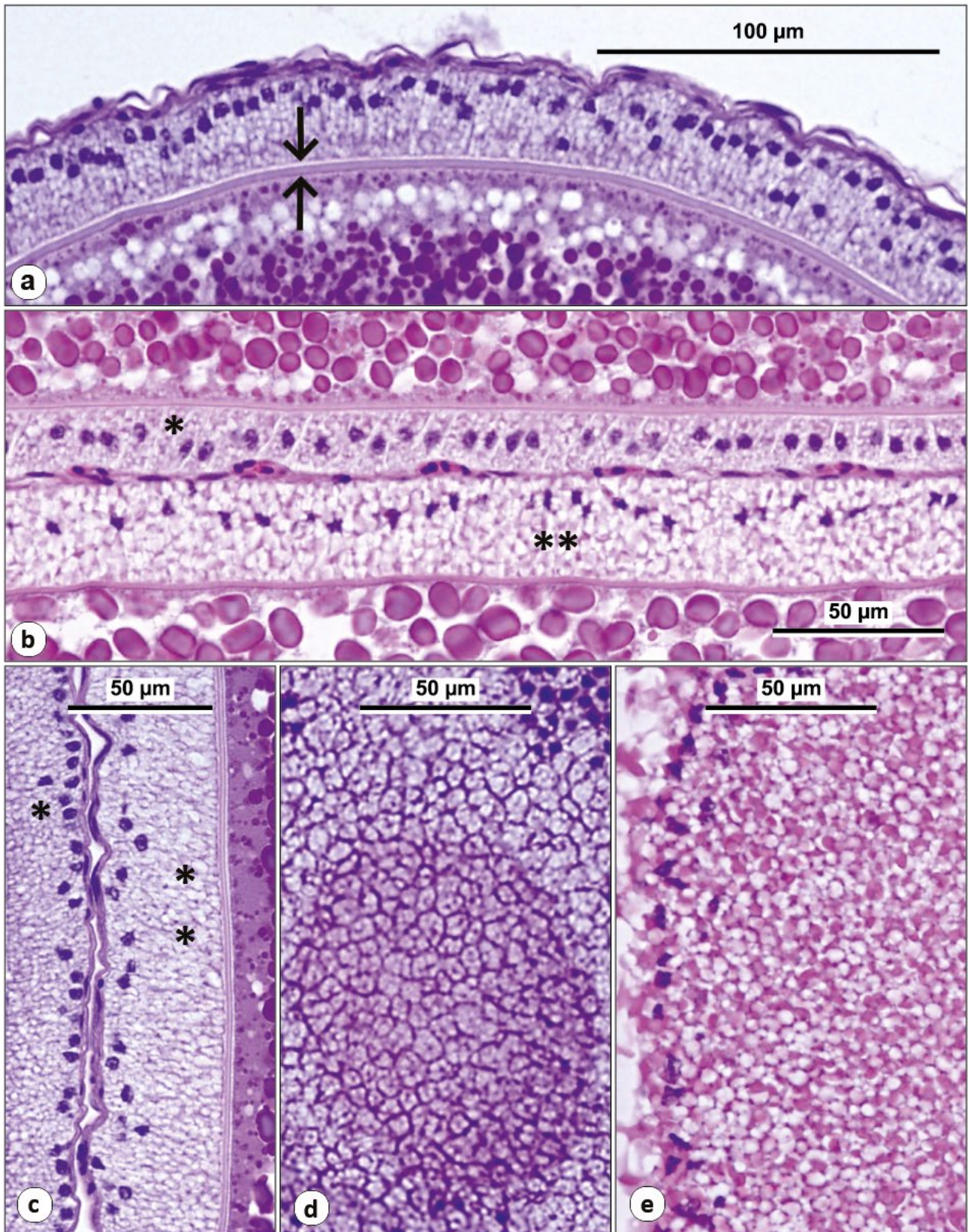


Fig. 5. Follicular cell layer enveloping oocyte. a) Zona radiata of the oocyte (defined by arrows) covered by follicular cell layer with nuclei close to the base membrane of this epithelium. b), c) Two follicular layers of oocytes lie opposite each other that differ in state of their transformation. (*) Represents an earlier stage of transformation. (**) Indicates a more advanced stage of transformation. d), e) Follicular cells are shown in different planes of sectioning; pronounced vacuolization seen in e). SMP a), c), d); SPT b); SPO e). H&E.

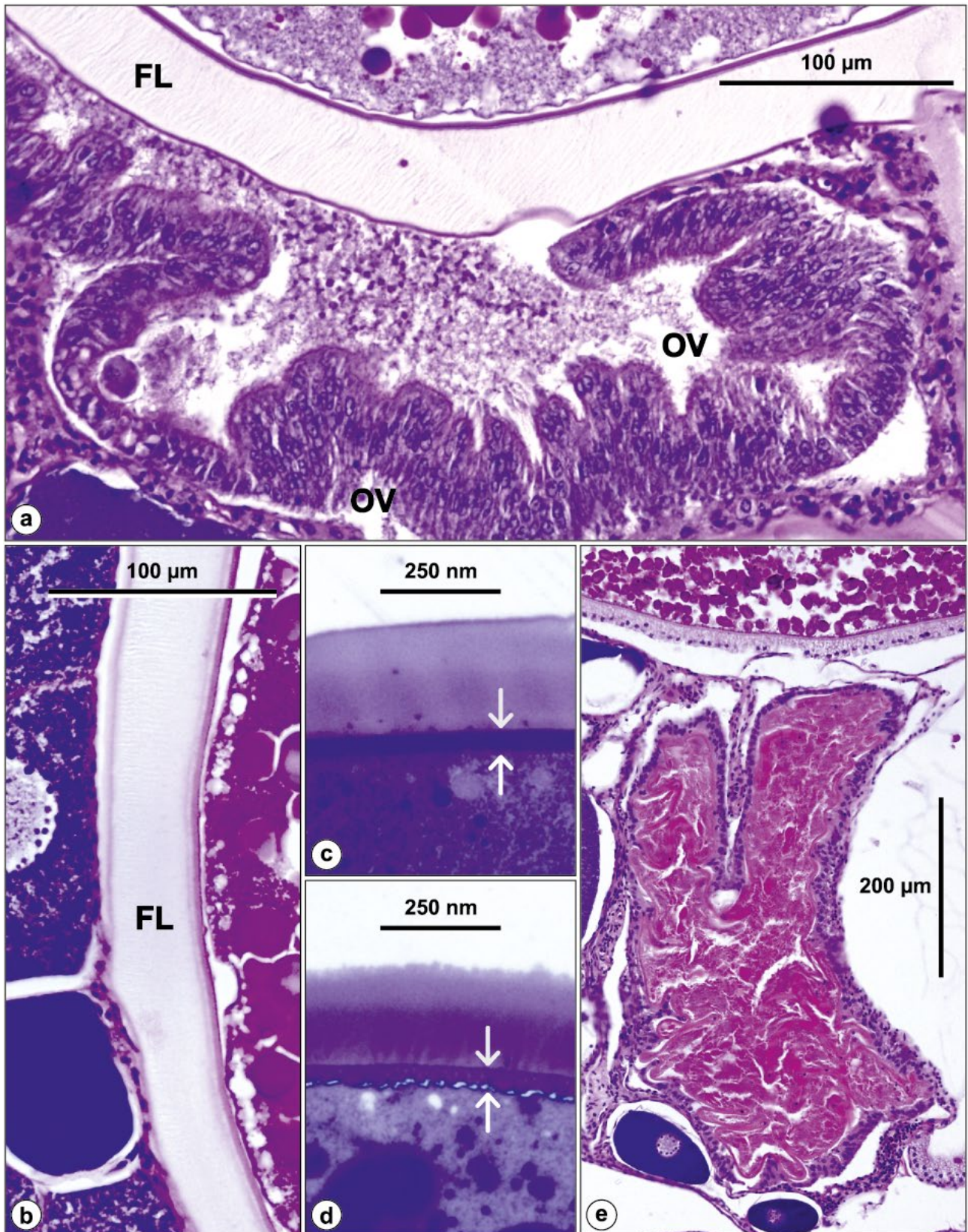


Fig. 6. Oocyte partially embedded in the oviduct (OV). a, b) The follicular cell layer (FL) transformed into an acellular homogeneous stratum. c, d) Oocytes of laboratory-reared *S. multipunctatus* prepared for artificial fertilization. Semi-thin sections show well-defined zona radiata, the thickness of which is defined by arrows. e) Atretic oocyte. SPO a), b); SMP c), d); SIR e). H & E.

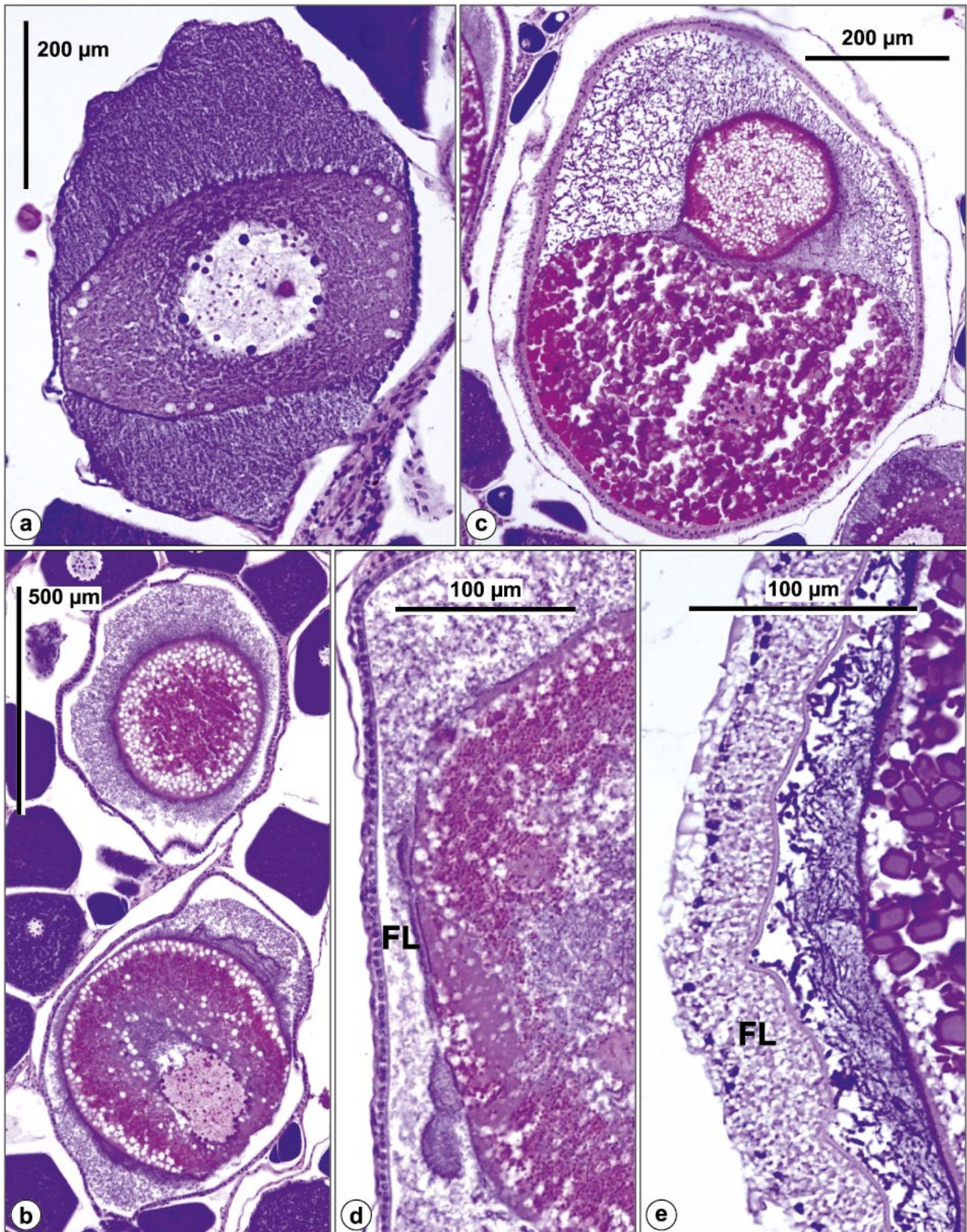


Fig. 7. Atypical findings of oocyte development. a) Aberrant previtellogenic stage of oogenesis with a cell-in-cell arrangement of stages closely resembling primary oocytes. b) Two aberrant oocytes resembling early vitellogenic stages of oogenesis. c) Aberrant oocyte with large aggregates of yolk droplets and vacuoles. d), e) Peripheries of two aberrant oocytes differing in the structure of the follicular layer (FL). SPO a), e); SIR (b-d). H & E.

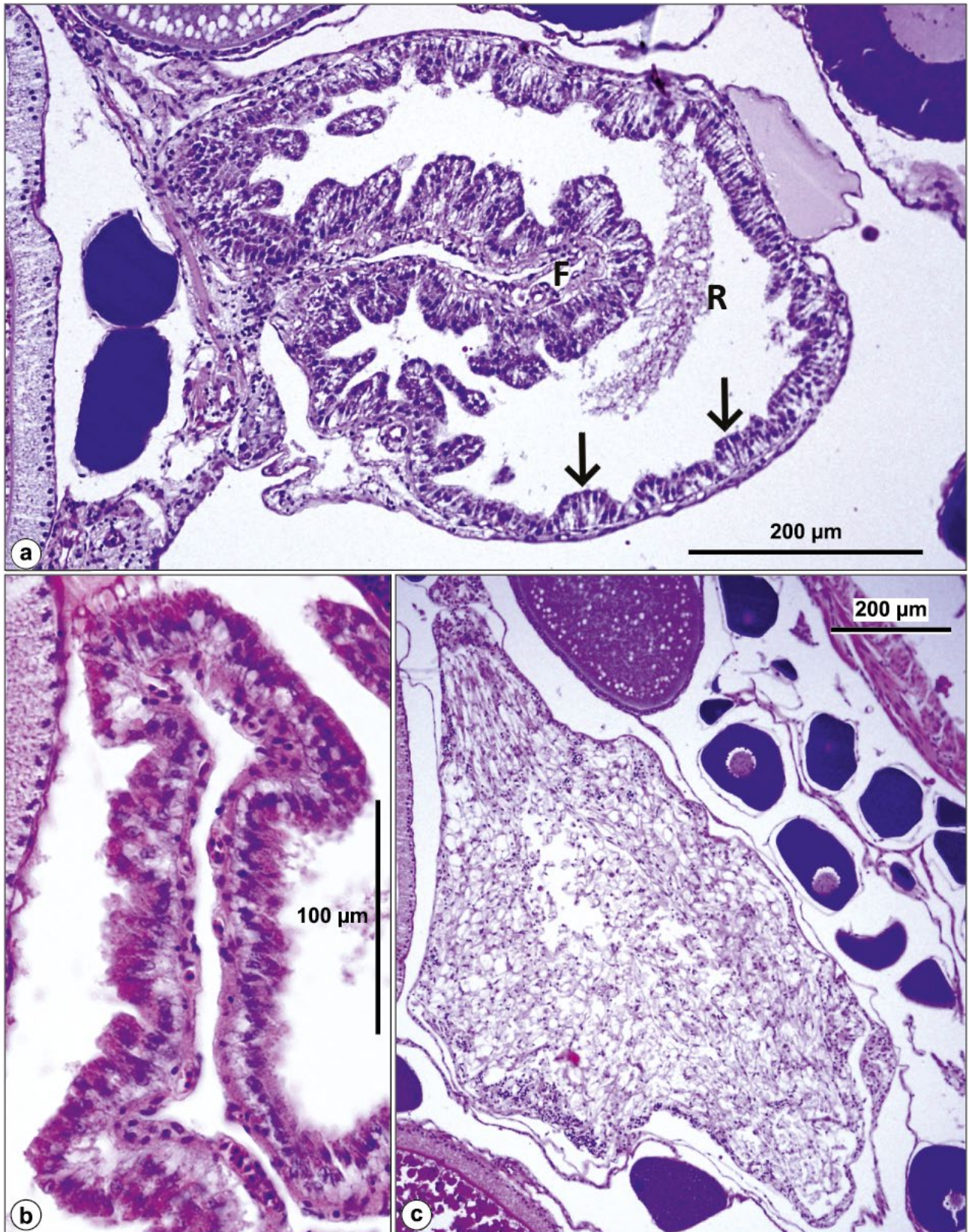


Fig. 8. Examples of postovulatory changes in ovaries. a) Oviduct of *S. multipunctatus* with fold (F) protruding into lumen, well visible lining epithelium (arrows) and luminal remnants of oocyte enveloping material (R). b) Fold of SPT oviduct with postovulatory changes of epithelium. c) Ovary of SPO with regressed tissue. Images of sections draw attention to changed structures, the origin of which is mostly difficult to determine. H & E.

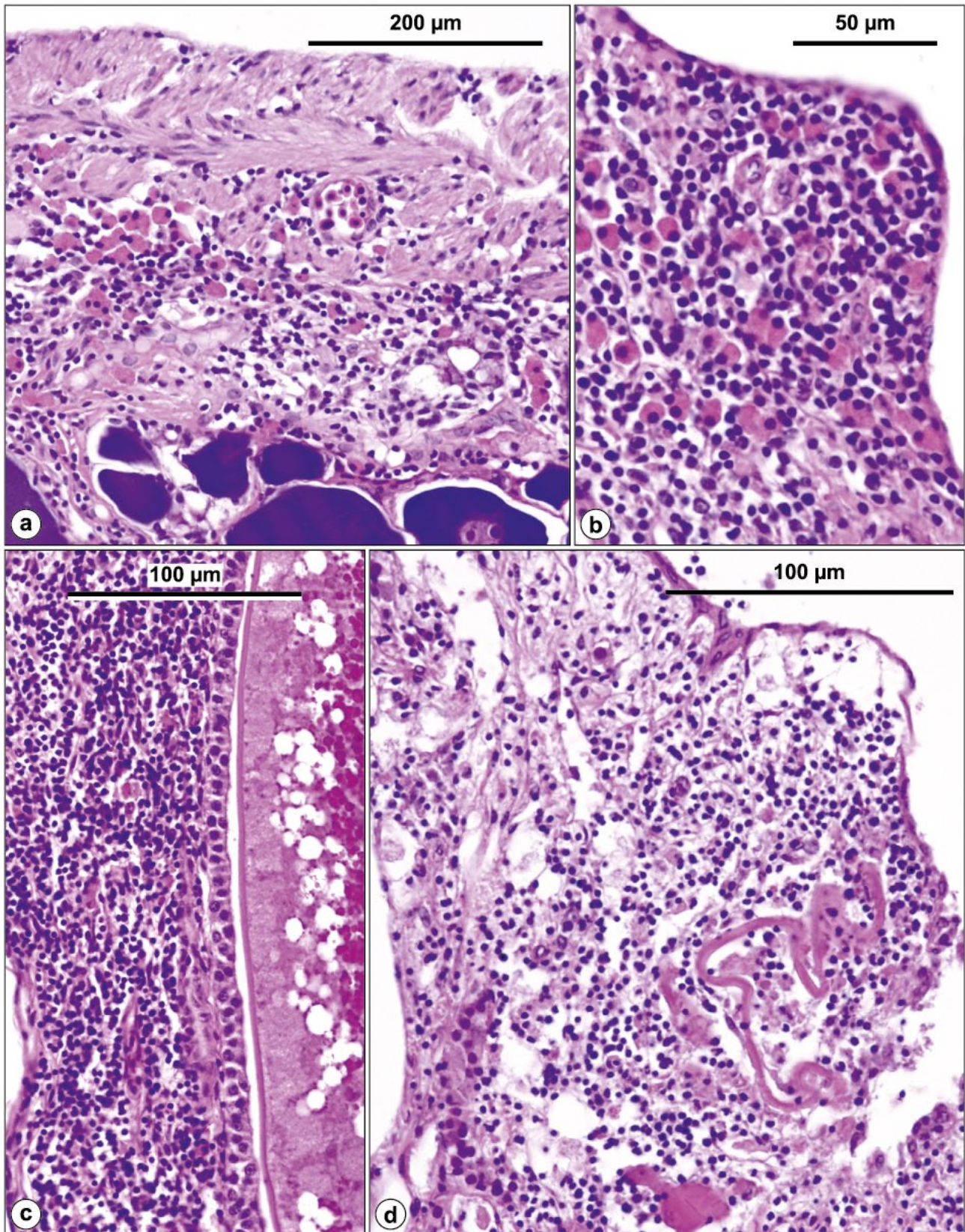


Fig. 9. Unusual cellularization in ovaries. a) Subthecal cell infiltrate containing lymphocytes and large eosinophilic cells resembling plasma cells. b) Detail of infiltrate present among developing previtellogenic stages. c) Dense lymphocytic infiltrate surrounding the vitellogenic stage of the oocyte. d) Connective tissue with supposed remnants of oocyte envelope densely infiltrated with lymphocytes. SPO a), b); SMP c); SIR d). H & E.

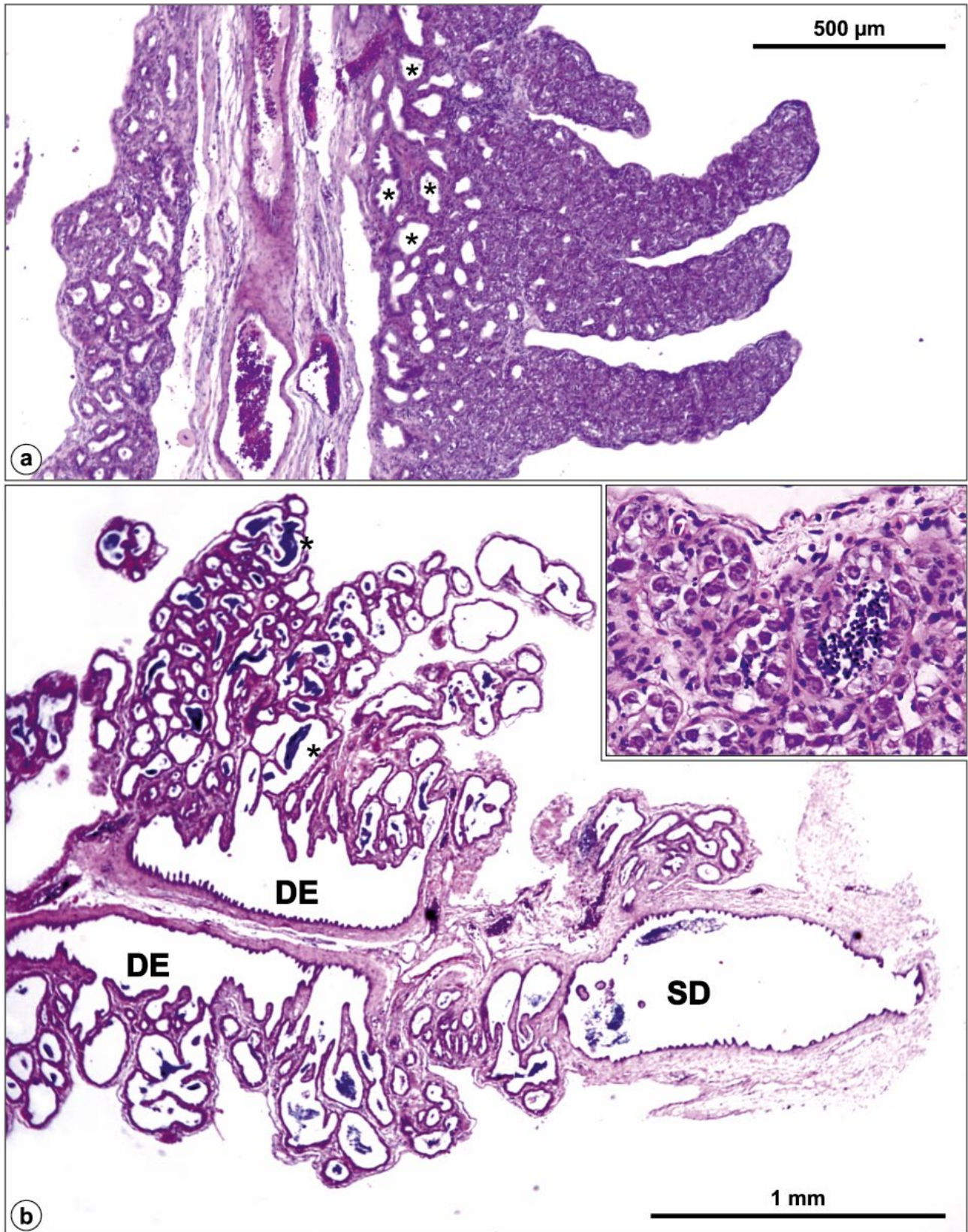


Fig. 10. Lobate architecture of *Synodontis* testes. a) Spermatogenic lobes of immature *S. polli* testes with collecting tubules (*) in overview; detail in b) inset. b) Overview of middle and caudal segment of *S. multipunctatus* testes. Tubules of individual lobes contain remnants of darkly stained spermatozoa (*). Main testicular ducts (DE) interconnected with collecting tubules of lobes. Posterior part of the efferent system, sperm duct (SD). H & E.

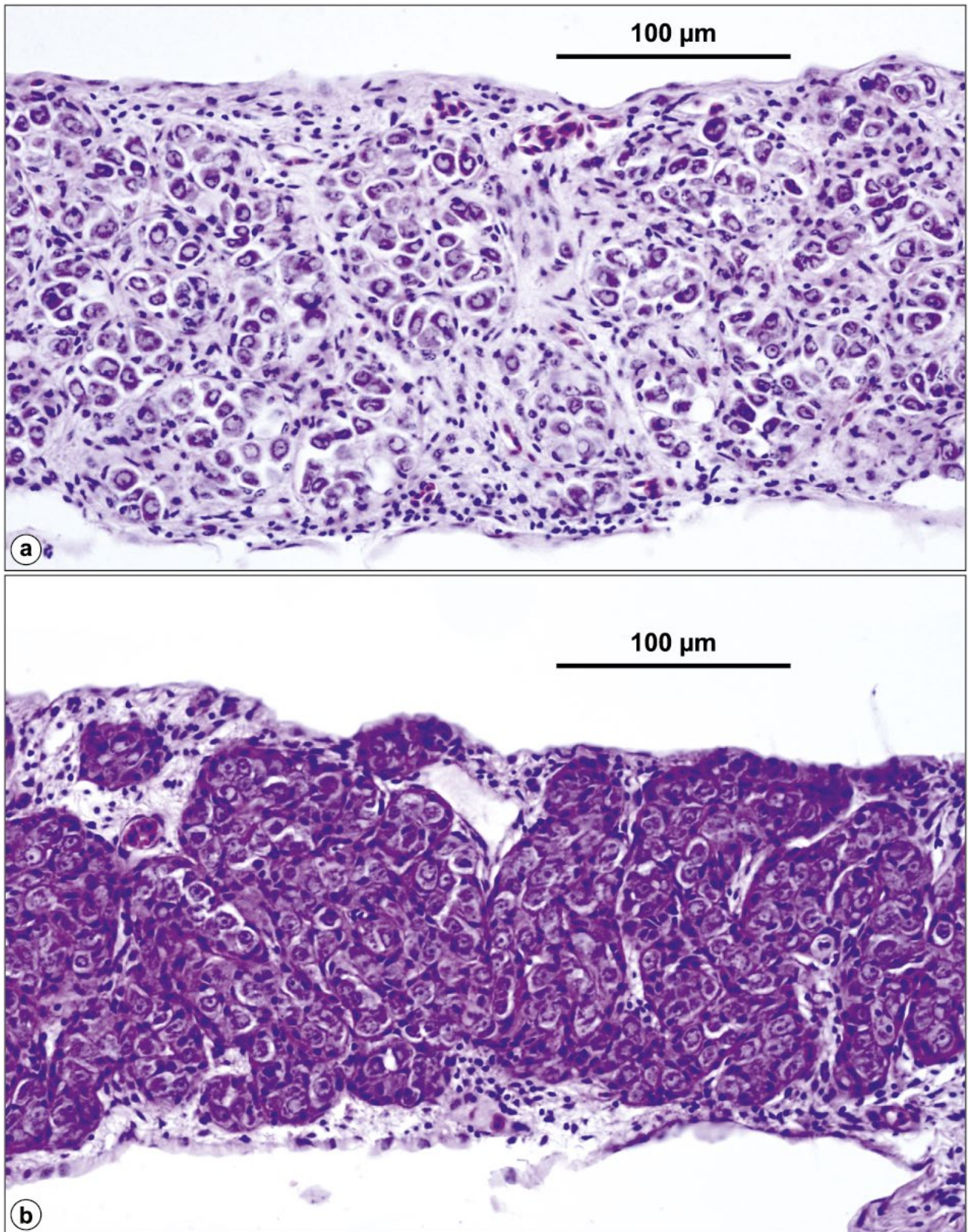


Fig. 11. Early phase of *Synodontis* spp. male gonad development. Testes of immature never spawned individuals. a) Longitudinal section through threadlike *S. polli* gonads presents isogenic clones of spermatogonia proliferating from germ cells, aggregated in nests and bounded by connective tissue. The tubular structure is not yet apparent. b) Early development of *S. irsacae* gonads. H & E.

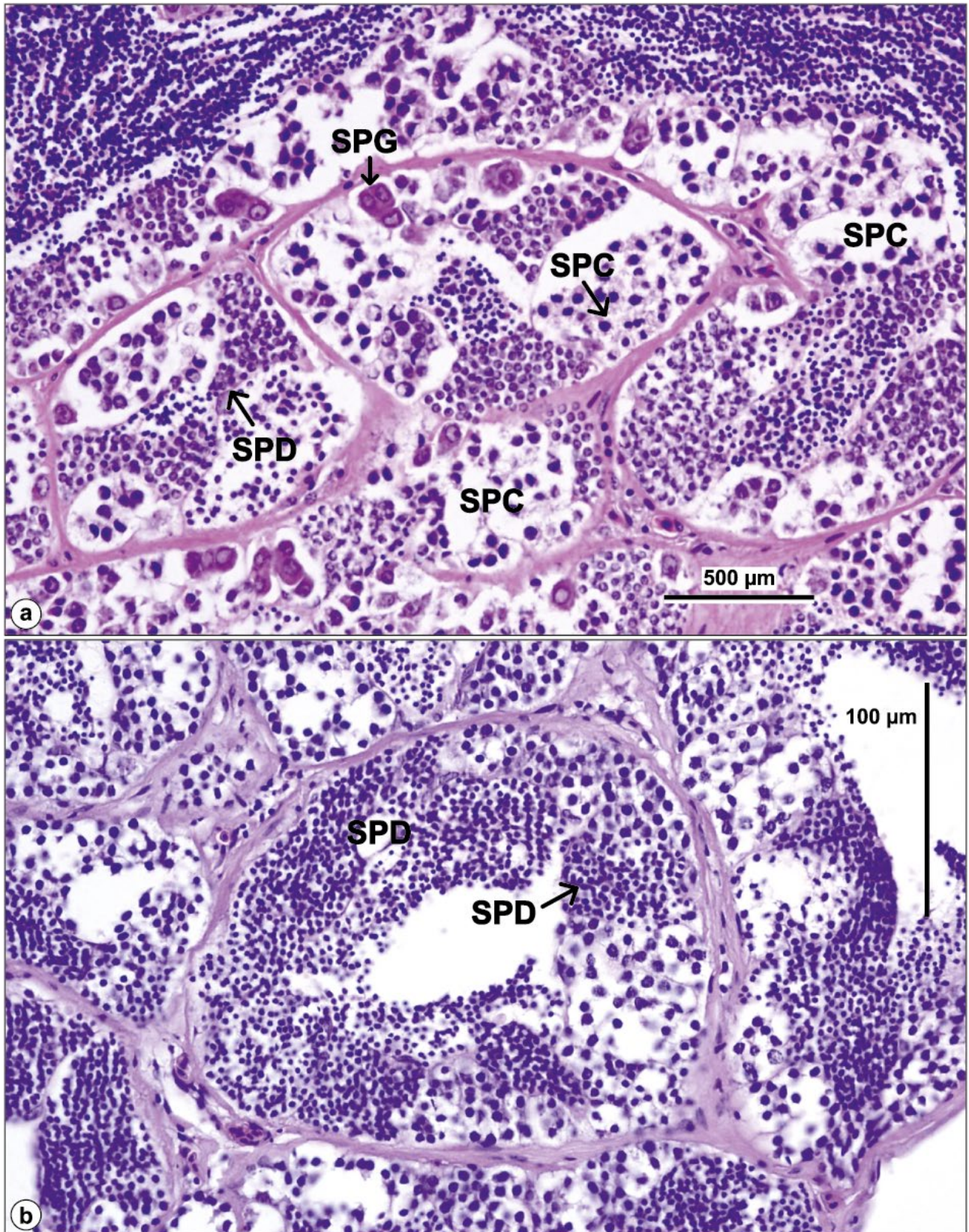


Fig. 12. Early stages of *Synodontis* spp. spermiogenesis. a) Seminiferous tubules in the testis of *S. irsacae* delimited by thick layers of connective tissue contain spermatogonia (SPG), clusters of spermatocytes (SPC) and spermatids (SPD). b) Seminiferous tubule of *S. polli* with small clusters of spermatocytes (SPC) and dominating clusters of spermatids (SPD). H & E.

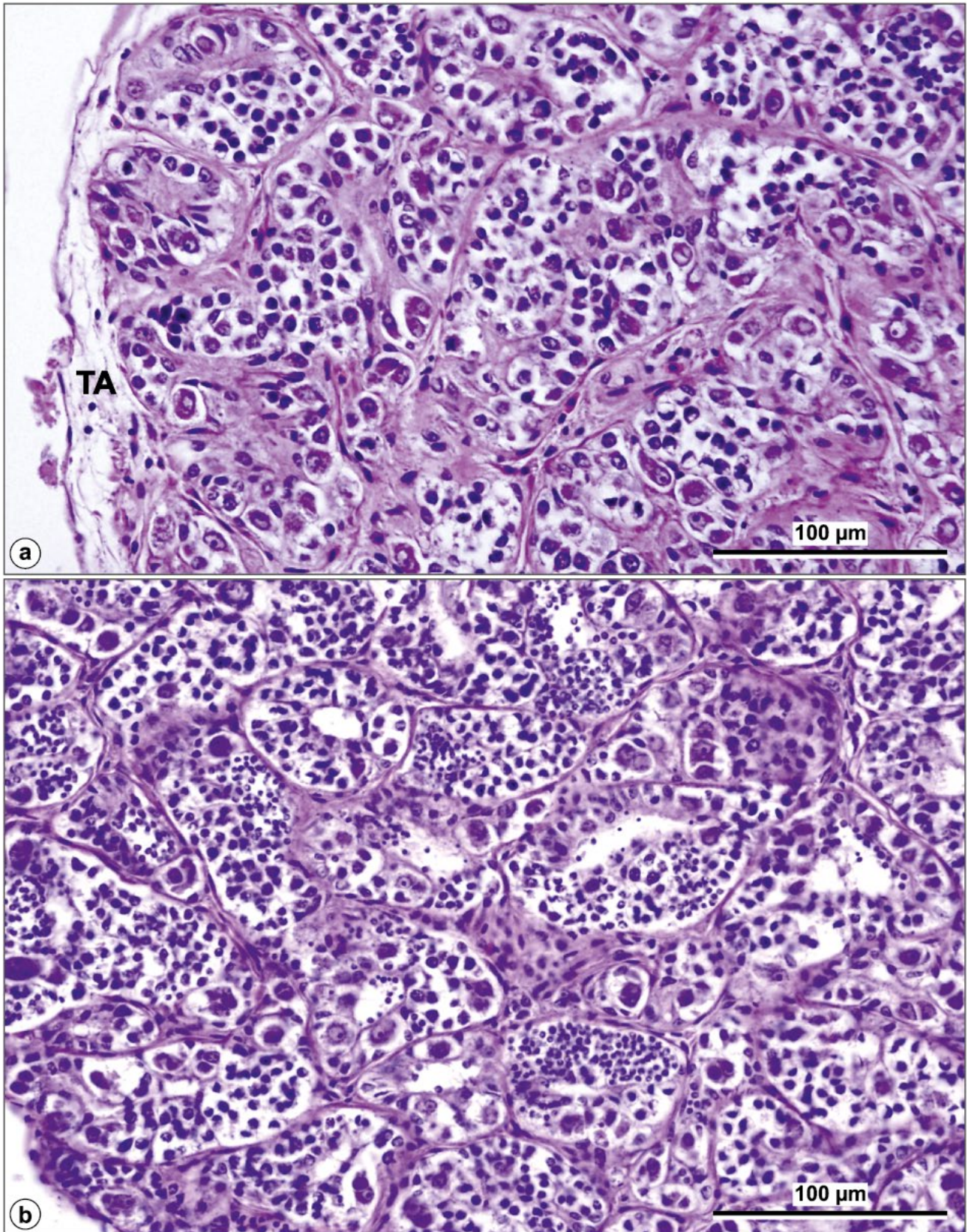


Fig. 13. Early stages of spermatogenesis in *Synodontis* spp. a) Testis of *S. irsacae* covered with tunica albuginea (TA) contains a pronounced proportion of connective tissue among clusters of spermatogenic stages. Spermatogonia and spermatocytes prevail. b) *S. melanostictus* testis parenchyma in a slightly advanced stage compared with a). The tubular arrangement of the seminiferous lobe is clearly indicated; tubules also contain spermatids. H & E.

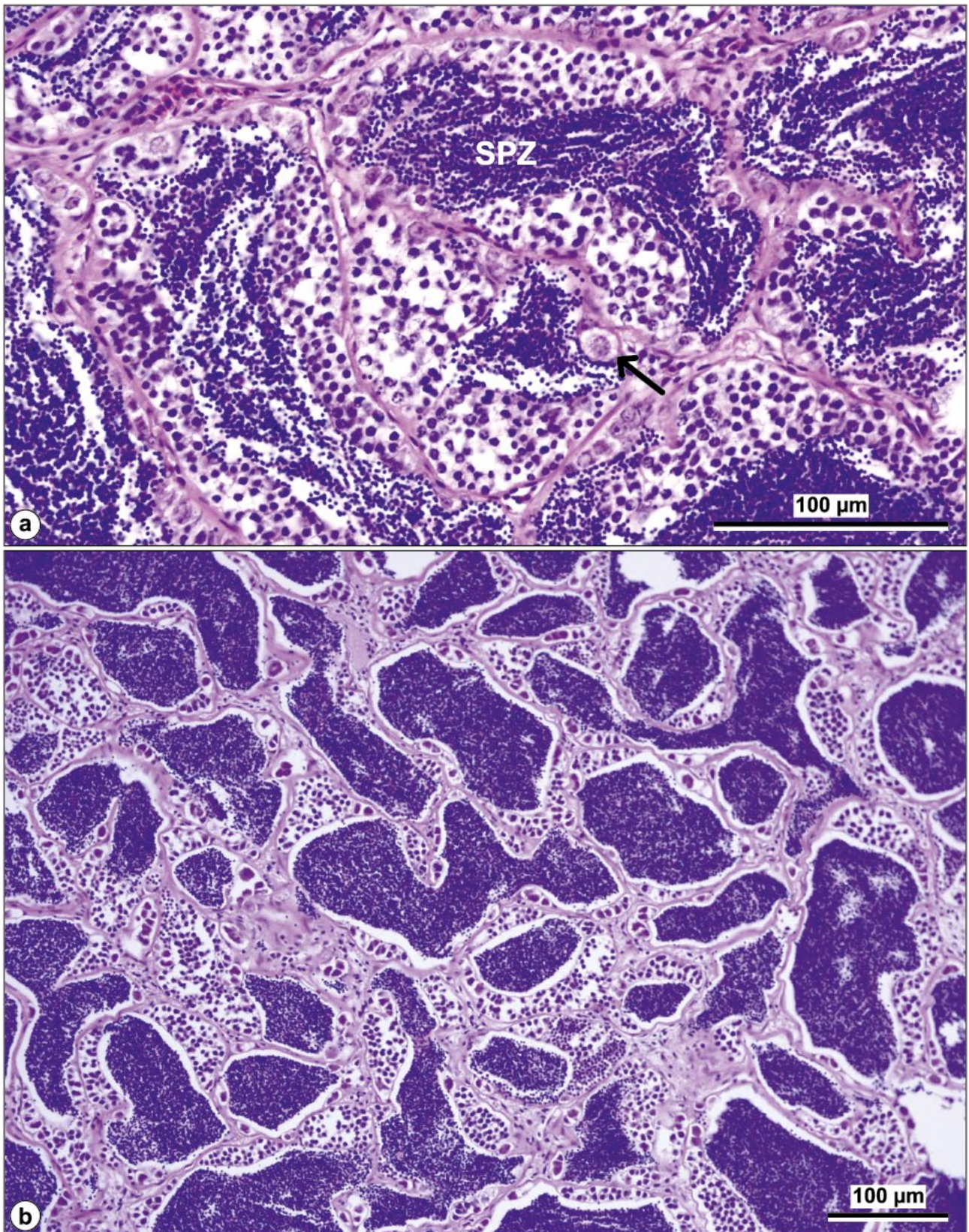


Fig. 14. Advanced stage of spermatogenesis in *Synodontis* spp. a) Seminiferous tubules in the testis of *S. petricola* with early developmental stages and accumulations of dark-stained spermatozoa (SPZ) in seminiferous tubules. Arrow marks Leydig cell in connective tissue. b) Parenchyma of *S. polli* testis in overview. Tubules filled with densely packed basophilic masses of spermatozoa are surrounded by earlier spermatogonial stages. H & E.

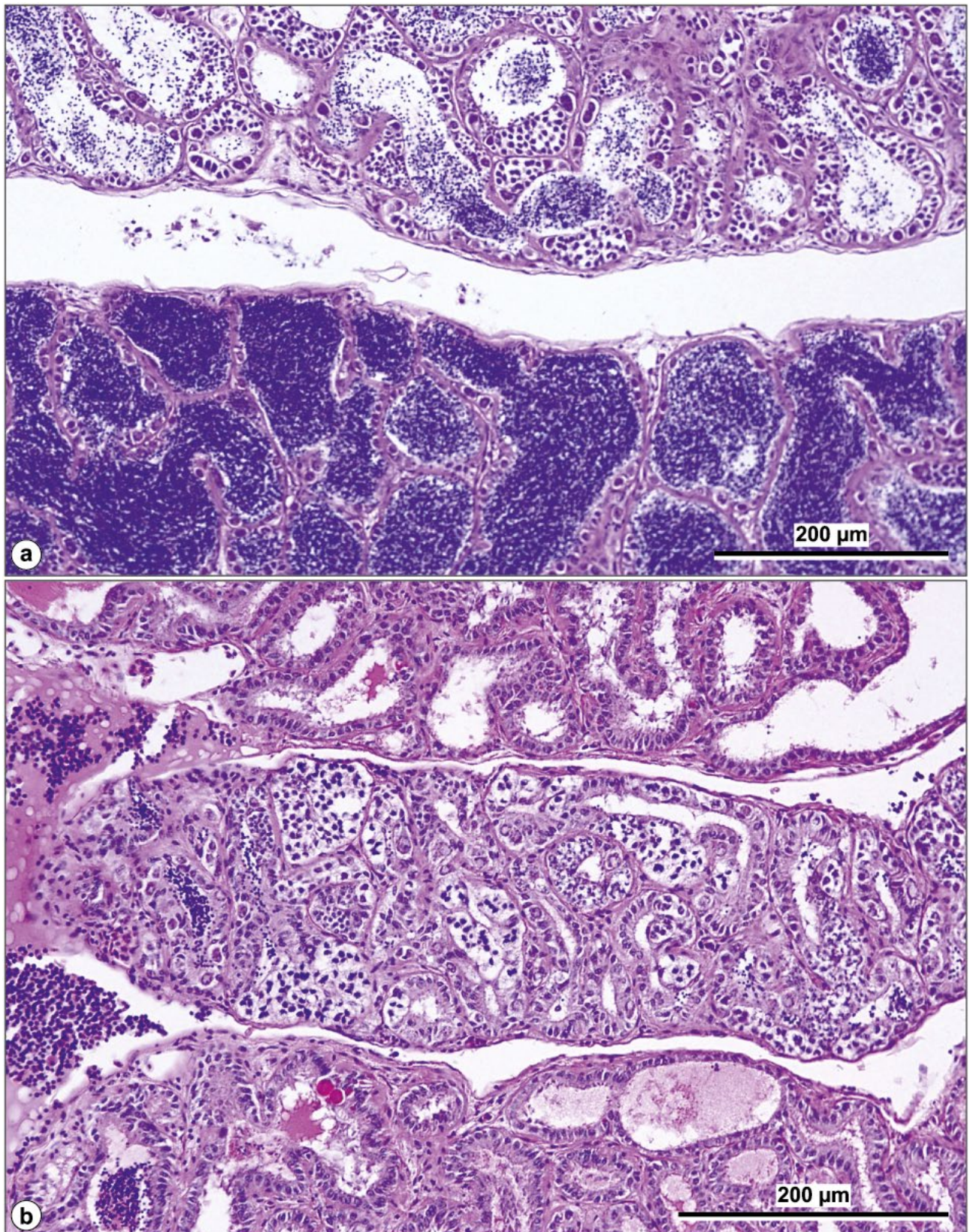


Fig. 15. Asynchronous spermatogenesis in testicular lobes of *Synodontis* spp. a) Two adjacent testicular lobes of *S. polli* differing in their spermatogenic phase. Earlier stages prevail in tubules of the upper lobe; spermatozoa fill the lumina of the tubules of the lower lobe. b) Section from testis of *S. irsacae*. Three neighbouring lobes demonstrate asynchrony in the function of individual lobes. H & E.

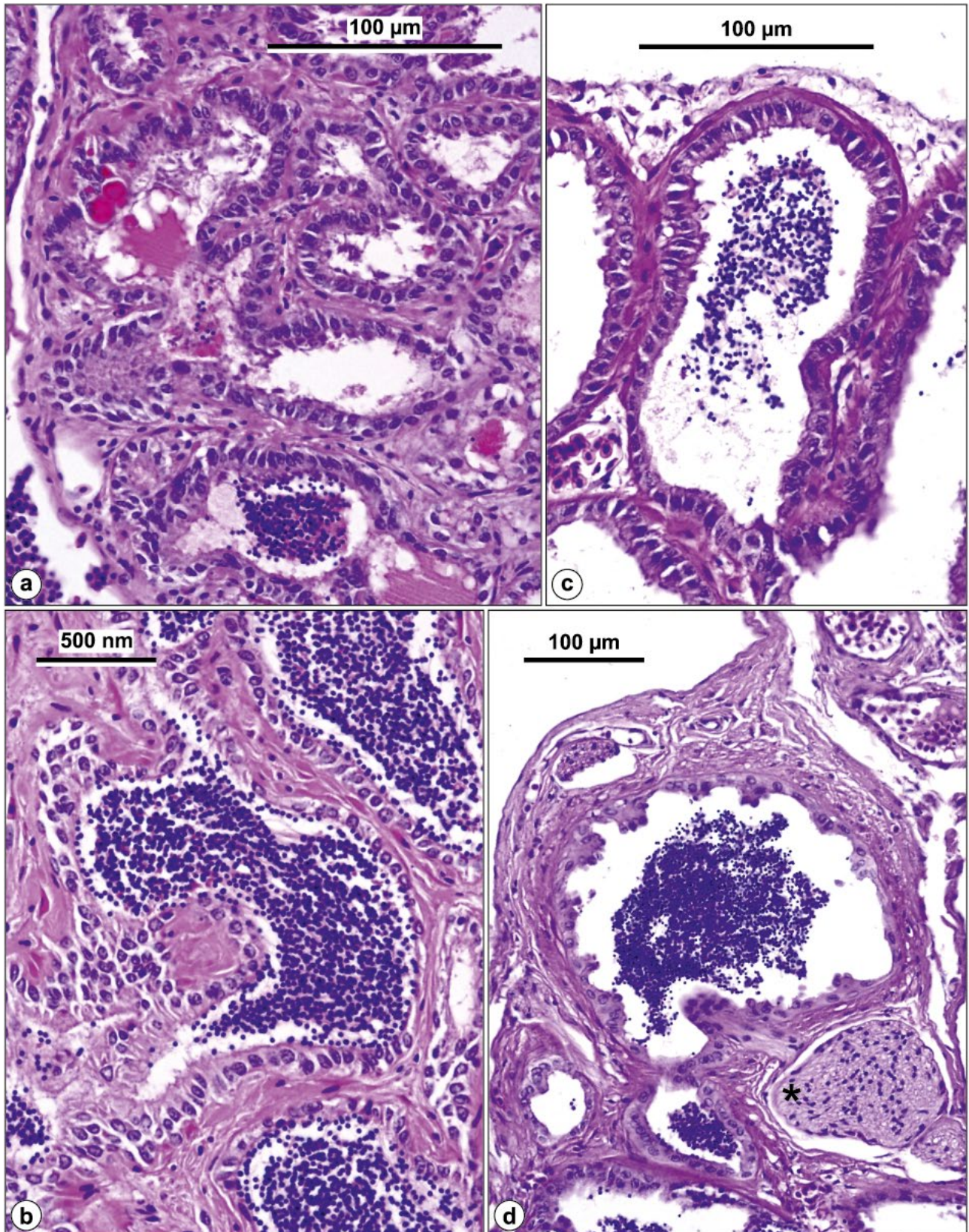


Fig. 16. Details of the efferent duct system in *Synodontis* testes. a), b) Efferent ducts of the spermiogenic lobe of *S. irsacae*, lined with cubic or columnar epithelial cells, contain acellular eosinophilic material, also reported as testicular plasma in a) and spermatozoa in a), b). c) Detail of efferent duct in spermiogenic lobe of *S. petricola*. d) Transverse section of SPO sperm duct with a massive bundle of nerve fibres (*) in close vicinity. H & E.

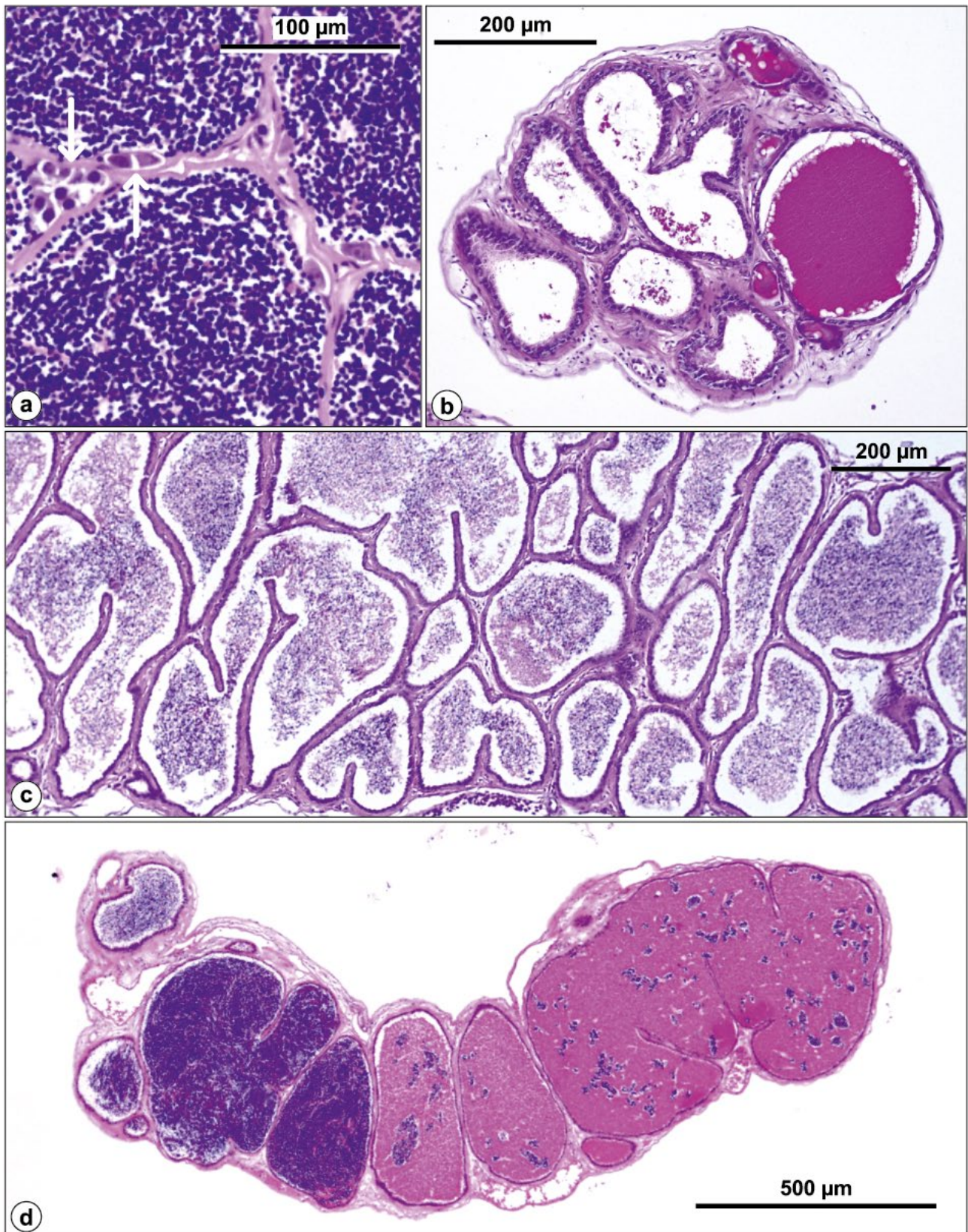


Fig. 17. Testes of *Synodontis polli*. a) Periphery of seminiferous tubules; compare with septa of multichambered SV in c). Arrows mark spermatogonia in tubules filled with spermatozoa. b) Efferent part of the lobe with ducts containing eosinophilic secretion. c) Chambers of SV storing spermatozoa at the same density. d) SV chambers differing in contents. Densely packed spermatozoa (left), eosinophilic SVP (right). H & E.

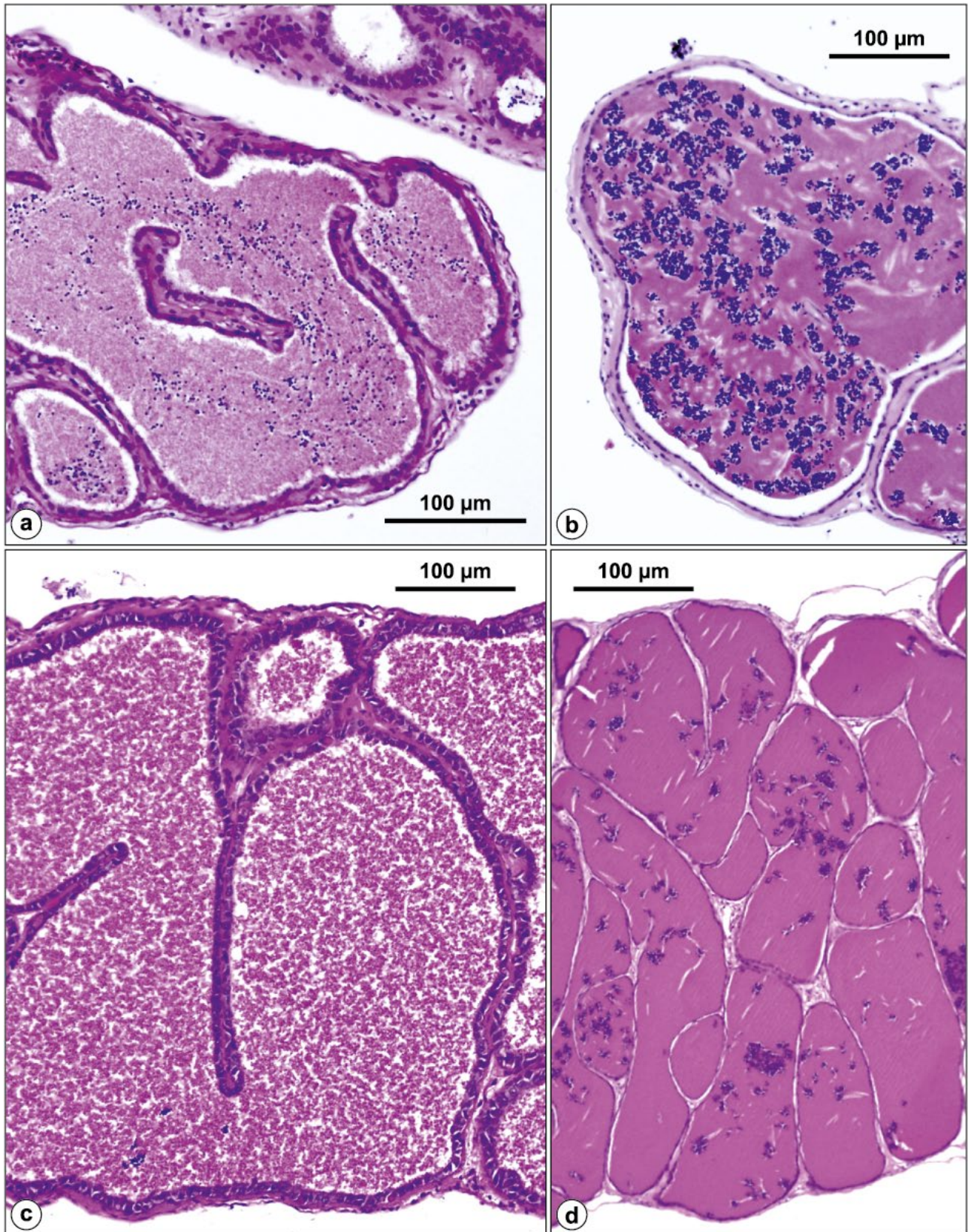


Fig. 18. Content of seminal vesicles in four *Synodontis polli* individuals. a) Vesicles are delimited by thin epithelium with eosinophilic material and sporadic basophilic cells (supposed spermatozoa). b) Large chamber in the tip of the vesicle with a mixture of eosinophilic secret and aggregates of spermatozoa. c) Precipitated acellular content free of spermatozoa. d) Eosinophilic dense masses with remnants of spermatozoa, no longer confined by epithelium. H & E.

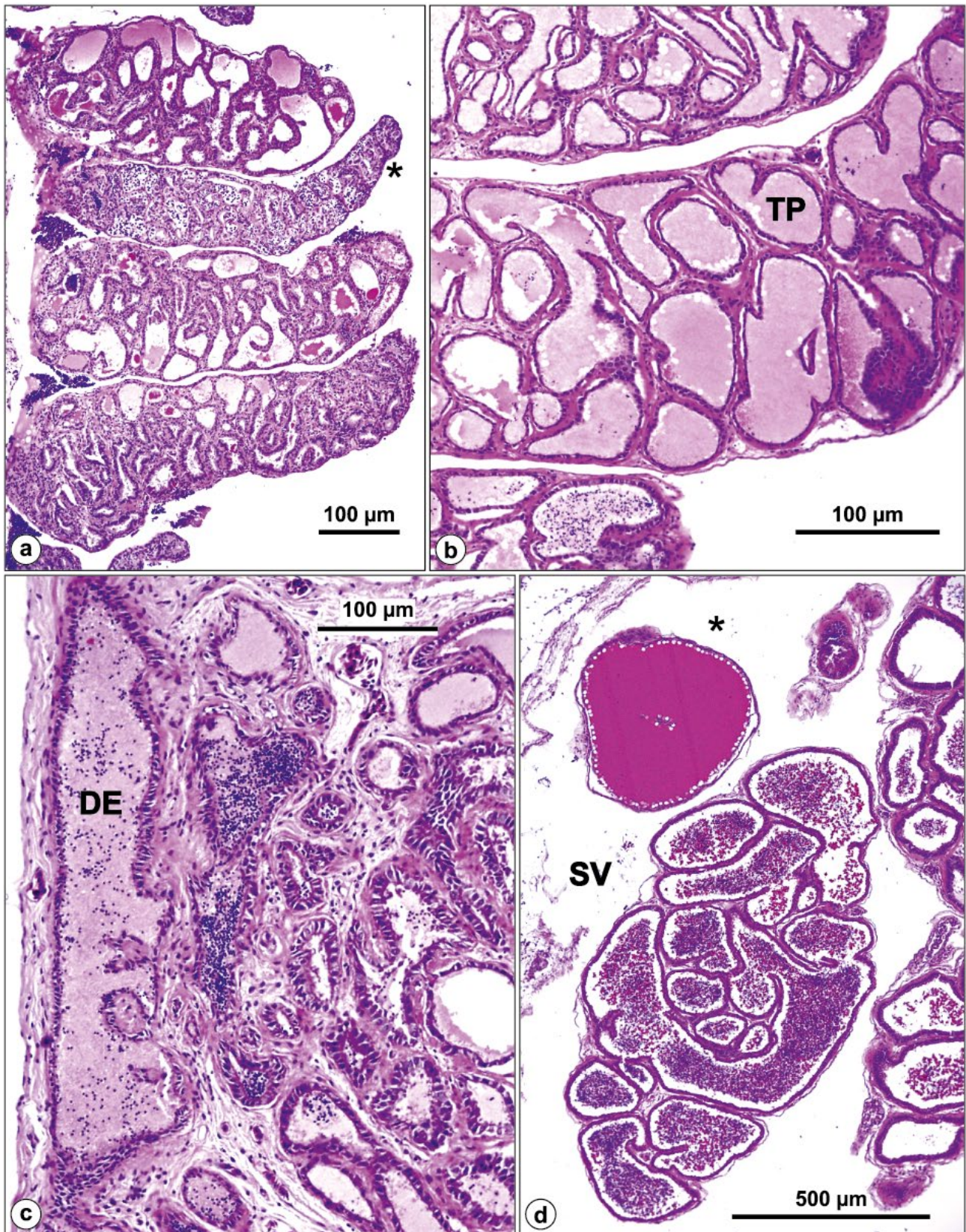


Fig. 19. Testes of *Synodontis irsacae*. a) Of four neighbouring testicular lobes, spermatogenesis occurs in one (*); homogeneous content reported as testicular plasma (TP) is shown in three. b) Acellular homogeneous content (TP) of three tubules a) shown in detail. c) Efferent part of the lobe presented in b) with the testicular duct (DE). d) Solitary tubule of supposed sperm duct gland (*) in transverse section close to SV. H & E.

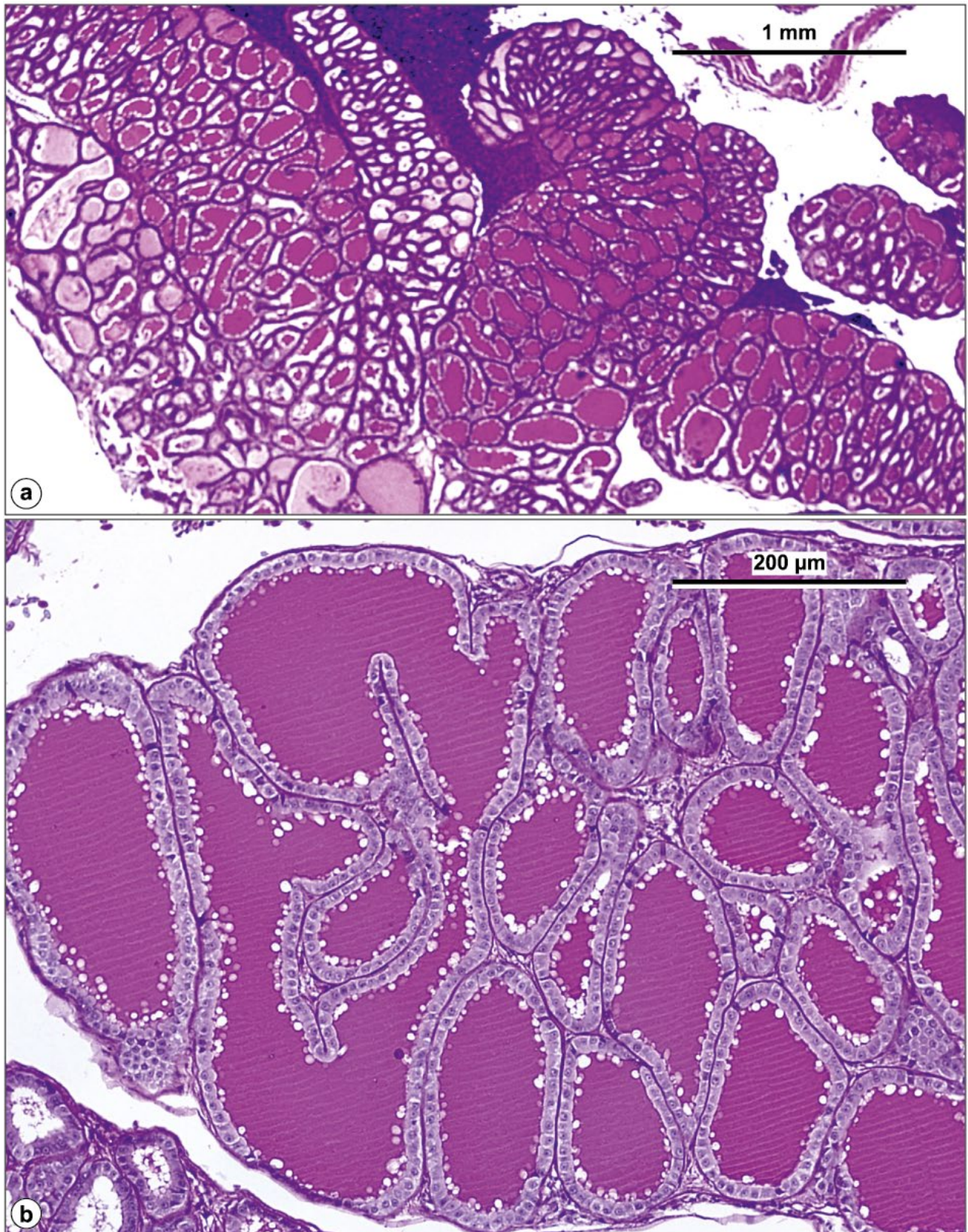


Fig. 20. Testes of *Synodontis melanostictus*. a) Posterior lobes/vesicles with a tubular structure containing homogeneous material slightly differing in the intensity of eosinophilia. b) Tubular structures of a) lined with simple cuboidal epithelium contain secretion, supposedly SVP, an essential component of seminal fluid. Intermingling and covering tissue is little pronounced. H & E.

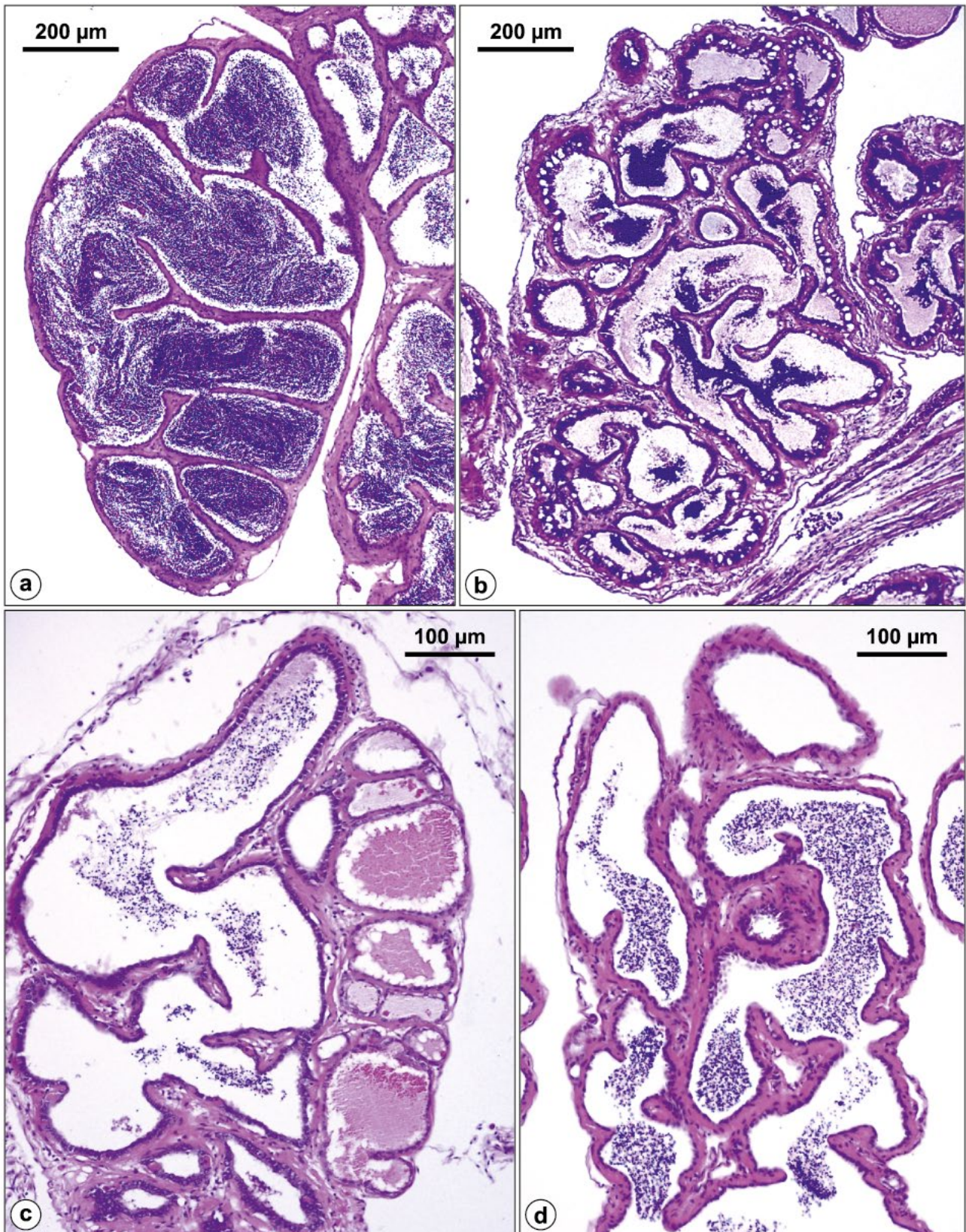


Fig. 21. Testes of *Synodontis multipunctatus*. a) Typical multichambered storage form of seminal vesicle densely packed with spermatozoa seen in laboratory-reared individual. b) Spermatozoa accumulating in secretory active tubules lined with vacuolated epithelium. Secretion is only slightly eosinophilic. c) Seminal vesicle with both storage chamber and secretory active tubules. d) Cross-section through seminal vesicle near sperm duct. H & E.

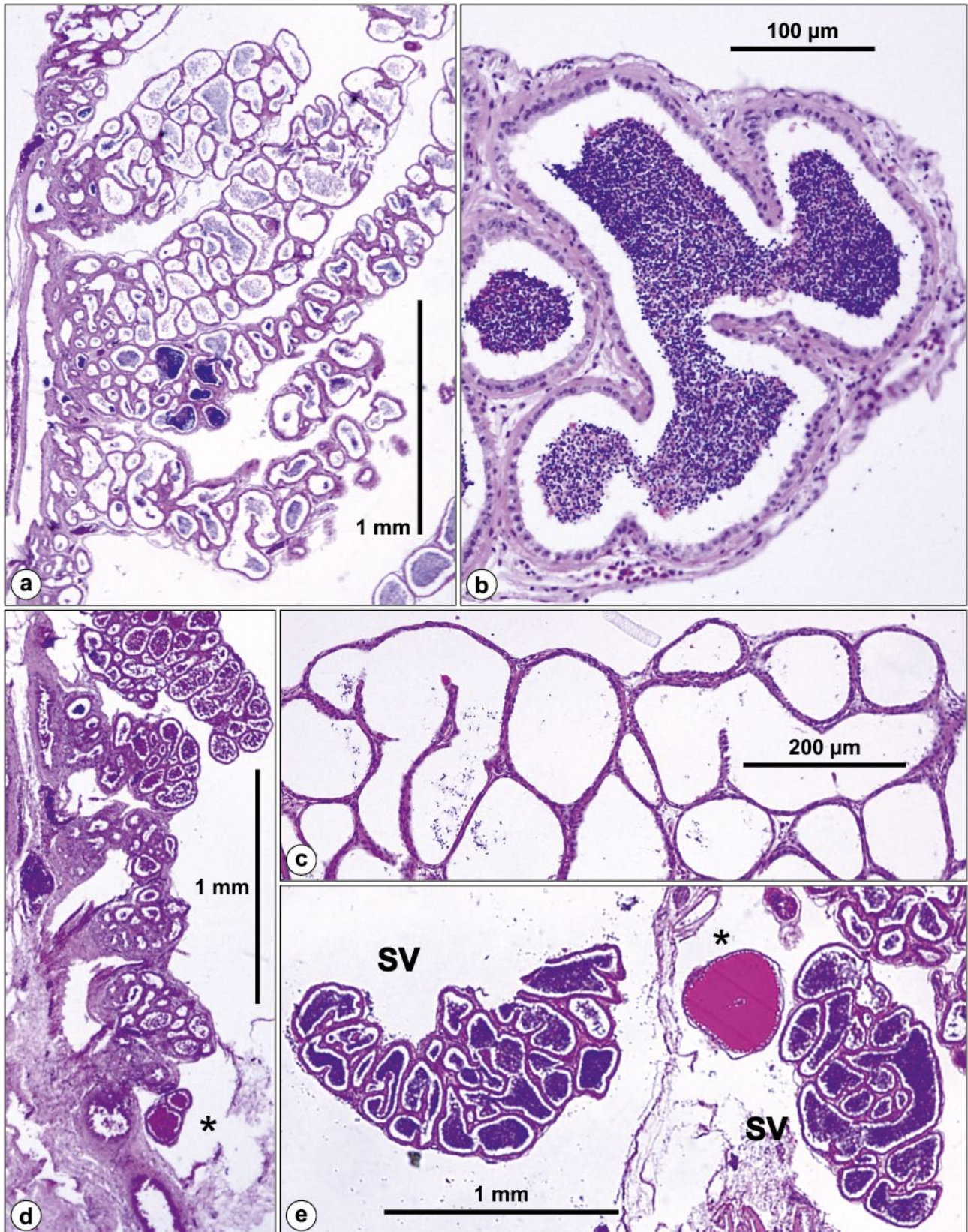


Fig. 22. Testes of *Synodontis petricola*. a) Neighbouring lobes/seminal vesicles in storage phase. b) Tip of seminal vesicle; chamber with densely packed spermatozoa is lined by cubic epithelium. c) Example of seminal vesicle with washed-out chamber contents. d) Posterior position of solitary tubules (*) with eosinophilic secretion. e) Solitary tubule filled with strongly eosinophilic secretion between the left and right seminal vesicle (SV). H & E.